Kinetic Analysis of the Action of Tissue Transglutaminase on Peptide and Protein Substrates

April Case and Ross L. Stein*

Laboratory for Drug Discovery in Neurodegeneration, Harvard Center for Neurodegeneration and Repair, 65 Landsdowne Street, Fourth Floor, Cambridge, Massachusetts 02139

Received April 10, 2003; Revised Manuscript Received June 10, 2003

ABSTRACT: Tissue transglutaminase (TGase) catalyzes transfer of γ-acyl moieties of Gln residues in peptides or protein substrates to either water or amine nucleophiles through an acyl−enzyme intermediate formed from initial acyl-transfer to an active site Cys residue. Natural substrates for this enzyme include proteins (e.g., tau, α-synuclein, and huntingtin) whose TGase-promoted polymerization may be causative in neurodegenerative diseases. As part of a program to find inhibitors of TGase, we have undertaken kinetic and mechanistic studies of the enzyme from guinea pig (gpTGase) and humans (hTGase). Key findings of this study include: (i) gpTGase-catalyzed transamidation of *Z*-Gln-Gly by Gly-OMe proceeds essentially as described above but with the involvement of substrate inhibition by Gly-OMe. This phenomena, resulting from the binding of nucleophile to free enzyme, appears to be a common feature of TGase-catalyzed reactions. (ii) Solvent deuterium isotope effects for hydrolysis of *Z*-Gln-Gly by gpTGase are $^{D}(k_c/K_m) = 0.45$ and $^{D}k_c = 3.6$. While the latter results from general catalysis of deacylation, the former originates purely from the reactant state, hydrogen fractionation factor of the active site thiol with no involvement of general catalysis of acylation. (iii) Studies of the transamidation of *N*,*N*-dimethylated casein by Gly-OMe and dansyl-cadaverine suggest a complex kinetic mechanism for both enzymes that reflects contributions from four reactions: Gln hydrolysis, intramolecular transpeptidation, intermolecular transpeptidation, and transamidation by added nucleophile.

Tissue transglutaminase (TGase)[1] (*1*, *2*) is a Ca^{2+}-dependent enzyme that stably cross-links intracellular proteins through the formation of isopeptide linkages between Gln and Lys residues (see Scheme 1). TGase not only catalyzes reactions of protein substrates but also the transamidation of Gln-containing peptides by a variety of simple primary amine nucleophiles. Principally on the basis of these latter model reactions, a chemical mechanism has emerged for TGase catalysis (*1*) that involves acyl-transfer to and from an active site nucleophile that is thought to be the sulfhydryl moiety of a Cys residue. According to this mechanism, the combination of TGase with a Gln-containing substrate to form a Michaelis-complex is followed by nucleophilic attack of the active site Cys to generate a covalent acyl−enzyme intermediate and an equivalent of ammonia. In the presence of a suitable primary amine, the acyl−enzyme undergoes aminolysis to regenerate free enzyme and the isopeptide product. In the absence of nucleophile, the acyl−enzyme will hydrolyze.

Scheme 1: Reaction Catalyzed by Tissue Transglutaminase

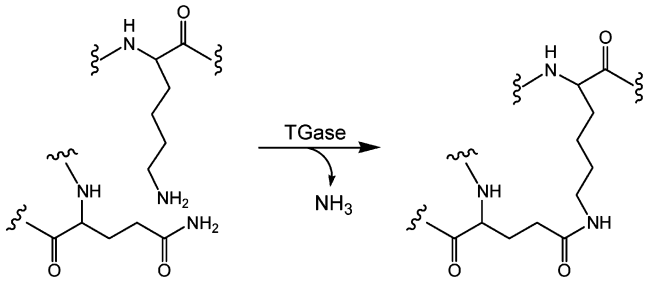

Our interest in TGase stems from its likely involvement in the development of a variety of neurodegenerative diseases (*3*−*5*), including Alzheimer's disease (*6*−*9*), Parkinson's disease (*4*, *10*), and Huntington's disease (*11*−*14*). These conditions are often associated with, and are perhaps causally linked to, the accumulation of aggregates of particular proteins. While the in vitro aggregation of these proteins can occur spontaneously, recent results from several laboratories suggest that the in vivo formation of these aggregates may be facilitated by the cross-linking activity of TGase (*10*, *15*, *16*).

As part of a program to find inhibitors of TGase, we have undertaken a study of the kinetics of reaction of this enzyme with protein substrates. In this paper, we report the results of our initial studies. To lay a conceptual foundation, we studied the TGase-catalyzed hydrolysis of prototype acyl-donor substrate *Z*-Gln-Gly as well as the substrate's transamidation by nucleophile Gly-OMe. With these studies as a backdrop, we conducted detailed kinetics studies on gpTGase- and hTGase-catalyzed reactions of protein substrate

* To whom correspondence should be addressed at Laboratory for Drug Discovery in Neurodegeneration, Harvard Center for Neurodegeneration and Repair, 65 Landsdowne Street, Fourth Floor, Cambridge, MA 02139. Phone: (617) 768−8651. Fax: (617) 768−8606. E-mail: rstein@rics.bwh.harvard.edu.

[1] Abbreviations: TGase, tissue transglutaminase (EC 2.3.2.13); gpTGase, guinea pig enzyme; hTGase, human enzyme; *N*-Me-casein or NMC, *N*,*N*-dimethylated casein; DSC, dansyl-cadaverine; cadaverine, 1,5-diaminopentane; FI, fluorescence intensity; Z-, carbobenzoxoyl; GDH, glutamate dehydrogenase; αKG, α-ketoglutarate.

10.1021/bi030084z CCC: $25.00 © 2003 American Chemical Society
Published on Web 07/18/2003

N,*N*-dimethylated casein in the absence and presence of nucleophiles Gly-OMe and dansyl-cadaverine. The kinetic mechanism that emerges from these studies is complex and, depending on reaction conditions, can reflect contributions from four reactions: Gln hydrolysis, intermolecular transpeptidation, intramolecular transpeptidation, and transamidation by added nucleophile.

MATERIALS AND METHODS

General. Buffer salts, *Z*-Gln-Gly, D_2O, casein (C-5890), *N*,*N*-dimethylated casein (C-9801), dansyl-cadaverine, α-ketoglutarate, NADH, and glutamate dehydrogenase were from Sigma Chemical Co. *p*-Nitrophenyl trimethyl acetate was from Aldrich. The experiments of this study were conducted at 30 °C in a pH 7.4 buffer with the following composition: 50 mM HEPES, 500 NaCl, 10 mM $CaCl_2$, 1 mM DTT.

Guinea Pig Liver TGase. gpTGase (Sigma T-5398) was purchased as a lyophilized powder and reconstituted to a protein concentration of 0.72 mg/mL in 50 mM HEPES, 500 mM NaCl, pH 7.4 containing 10% glycerol and stored at −20 °C. Concentration of active sites was determined using *p*-nitrophenyl trimethyl acetate as titrant. Each day's kinetic experiments were conducted with a freshly thawed aliquot of stock enzyme.

Expression and Purification of Human TGase. The expression clone for human 6His-tagged TGase was a gift from Dr. Chaitan Khosla (Stanford University) and the method that follows for the expression and purification of this enzyme is essentially as reported (*17*). Sixty milliliters of LB containing 50 μg/mL kanamycin was inoculated with glycerol stock of the expression clone and the bacteria were allowed to grow overnight at 37 °C. Twenty milliliters of culture was added per liter of LB containing 50 μg/mL kanamyin. This was incubated on a shaker (250 rpm, 37 °C) until OD_{600} was 0.6 at which time flasks were cooled to room temperature and expression was induced with 250 μM IPTG. After an overnight incubation of the sample at room temperature, these cultures were centrifuged at 2800*g* for 15 min (4 °C) and the recovered bacterial pellets were suspended in a pH 7.5 solution of 50 mM Tris, 300 mM NaCl, and 5 mM imidazole. This suspension was then subjected to microfluidization at 10 000 psi to lyse the bacteria. The lysate was centrifuged at 9000*g* for 40 min (4 °C), and the supernatant was collected and adjusted with Ni−Sepharose to a level of 1 mL of gel/50 mL of supernatant. To allow optimum binding of 6His-tagged TGase to Ni−Sepharose, the slurry was gently rocked for 1.5 h (4 °C). The gel was collected by centrifugation at 800*g* for 5 min (4 °C) and then washed batch-wise as follows: 3 × 10 mL, 10 mM imidazole in 50 mM Tris, 300 mM NaCl, pH 7.5; 2 × 6 mL, 25 mM imidazole in 50 mM Tris, 300 mM NaCl, pH 7.5; 1 × 5 mL, 50 mM imidazole in 50 mM Tris, 300 mM NaCl, pH 7.5; and 1 × 4 mL, 500 mM imidazole in 25 mM Tris, 150 NaCl, pH 7.5. From the final elution, 3.7 mL of 0.23 mg/mL was recovered. This solution was adjusted with glycerol to 10% and stored as 250 μL aliquots at −80 °C.

Kinetic Methods − TGase-Catalyzed Hydrolysis and Transamidation of Z-Gln-Gly. Ammonia production that results from the hydrolysis of *Z*-Gln-Gly to *Z*-Glu-Gly is monitored using a GDH-coupled assay essentially as described by Day and Keillor (*18*). In a typical kinetic run, 980 μL of assay buffer containing 6 mM αKG, 0.33 mM NADH, and a predetermined concentration of *Z*-Gln-Gly (0.5 mM ≤ [*Z*-Gln-Gly] ≤ 10 mM) is added to a 1-mL cuvette, and the cuvette placed in the jacketed cell holder of a Perkin-Elmer Lambda 20 spectrophotometer. A total of 10 μL of a 1750 U/mL stock solution of GDH is next added to the cuvette to achieve a final [GDH] of 20 U/mL. After a stable baseline at 340 nm is established and the solution has come to thermal equilibrium at 30 °C, an aliquot of stock TGase is added to the cuvette to initiate the reaction. Reaction progress is monitored by the decrease in absorbance at 340 nm ($\Delta\epsilon_{340} = -6200$) that accompanies oxidation of NADH. For each kinetic run 100−3000 data points, corresponding to (time, absorbance) pairs, are collected by a PC interfaced to the spectrophotometer.

Isopeptide bond formation between *Z*-Gln-Gly and the nucleophile Gly-OMe is also monitored as the production of ammonia essentially as described above for the hydrolysis of *Z*-Gln-Gly. For these experiments, NADH concentration is increased to 0.66 mM.

Kinetic Methods − Action of TGase on Casein or N-Me-Casein. Reaction of TGase with casein or *N*-Me-casein produces one molecule of ammonia per enzymatic turnover. During the course of these reactions, ammonia can be monitored essentially as described above. In these experiments, small aliquots of a concentrated stock solution of casein (200 μM in assay buffer) or *N*-Me-casein (500 μM in assay buffer) are added to reaction solutions containing 6 mM αKG, 0.33 mM NADH, and 40 U/mL GDH in assay buffer. Reactions are initiated by addition of TGase.

These reactions, as well as those using *Z*-Gln-Gly, are also studied using a microplate spectrophotometer. This allowed multiple reactions to be followed simultaneously with little decrease in data quality relative to the Perkin-Elmer Lambda 20 spectrophotometer.

Kinetic Methods − TGase-Catalyzed Incorporation of Dansyl-Cadaverine into N-Me-Casein. TGase-catalyzed isopeptide bond formation between dansyl-cadaverine and Gln residues of *N*-Me-casein is accompanied by an increase in dansyl fluorescence that can be monitored continuously at 500 nm ($\lambda_{ex} = 330$ nm). In a typical assay, 1.97 mL of assay buffer is added to a 3-mL fluorescence cuvette containing a stir bar, and the cuvette placed in the jacketed cell holder of a Hitachi F4500 fluorometer. Stirring is maintained throughout the kinetic experiment and temperature is held constant 30 °C by a circulating water bath. Small aliquots of stock solutions of *N*-Me-casein (500 μM in assay buffer) and dansyl-cadaverine (500 mM) are next added to the cuvette. To initiate the reaction, a aliquot of TGase stock solution is added. For each kinetic run 100−3000 data points, corresponding to (time, fluorescence) pairs, are collected by a PC interfaced to the fluorometer.

These reactions are also studied using a Molecular Devices Gemini XS microplate spectrofluorometer. This allowed multiple reactions to be followed simultaneously with little decrease in quality of data relative to the Hitachi F4500 fluorometer.

TGase-Catalyzed Cross-Linking of Casein or N-Me-Casein. In these experiments, 50 μM casein or *N*-Me-casein was incubated with 13 μM gpTGase at 30 °C in a pH 7.4 buffer having composition: 50 mM HEPES, 500 mM NaCl,

Scheme 2: Mechanistic Proposal for Reaction of Tissue Transglutaminase with Minimal Substrates *Z*-Gln-Gly and Gly-OMe

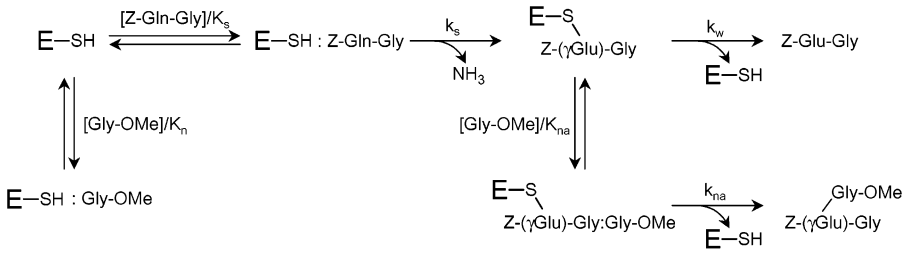

10 mM $CaCl_2$, and 1 mM DTT. At predetermined times, 100 μL aliquots of the reaction solution were taken and immediately mixed with an equal volume of 2× SDS sample running buffer. Separation of proteins by SDS−PAGE was performed using the Novex X Cell II minigel apparatus. An 18% Tris-glycine precast gel was used. Proteins were stained with Coomassie blue dye for visualization.

Curve Fitting and Simulations. Fitting of progress curves and production of simulations were accomplished using the program Scientist, MicroMath Scientific Software (available through Echoscan, Inc. (http://www.echoscaninc.com), P. O. Box 2111, Niagara Falls, ON, Canada, L2E 672).

RESULTS

TGase-Catalyzed Reactions of Z-Gln-Gly. Our studies of reactions of *Z*-Gln-Gly were conducted using a GDH-coupled assay (*18*) that allows continuous measurement of the ammonia that is produced by the action of TGase on its substrates (see Scheme 1). In this assay, ammonia serves as substrate for GDH to promote the αKG-dependent oxidation of NADH to NAD^+ ($\Delta\epsilon_{340} = -6{,}220$). Consistent with the general theory for coupled enzyme assays (*19*), progress curves for the disappearance of NADH are characterized by (i) a pre-steady-state lag phase of duration that is inversely proportional to the concentration of the coupling enzyme GDH, and (ii) steady-state velocities, v_{ss}, that are linearly dependent on the concentration of primary enzyme TGase (data not shown).

In preliminary experiments (data not shown), we determined steady-state kinetic parameters for the gpTGase-catalyzed hydrolysis of *Z*-Gln-Gly as well as for the gpTGase-catalyzed transamidation of *Z*-Gln-Gly at a single concentration (3 mM) of amine nucleophile Gly-OMe. For the former reaction, the dependence of steady-state velocity on substrate concentration (0.5 mM ≤ [*Z*-Gln-Gly] ≤ 10 mM) was hyperbolic and allowed calculation of the following best-fit parameters according to the Michaelis−Menten equation: $k_c = 0.17\ s^{-1}$, $K_m = 1.8$ mM, and $k_c/K_m = 96\ M^{-1}\ s^{-1}$. In contrast, for Gly-OMe-promoted transamidation, we observed a linear dependence of v_{ss} on *Z*-Gln-Gly concentrations that again ranged from 0.5 to 10 mM, indicating that $(K_m)_{app}$ must be greater than 10 mM in the presence of 3 mM Gly-OMe. The linear dependence of v_{ss} on [*Z*-Gln-Gly] allowed calculation of $(k_c/K_m)_{app}$ as the slope of this relationship and was found to equal $72\ M^{-1}\ s^{-1}$, a value that is slightly reduced relative to k_c/K_m for the simple hydrolysis reaction. These results are consistent with the standard acyl-transfer mechanism that has been proposed for TGase (*1*). According to this mechanism, the acyl−enzyme intermediate can undergo reaction with either water, to form a Glu-containing product, or with an amine nucleophile, to form an isopeptide product. If formation of the acyl−enzyme is rapid relative to its hydrolysis, then reaction of the acyl−enzyme with an amine nucleophile will provide a more rapid pathway for enzyme turnover and result in apparent values of k_c and K_m that are larger than those values for the simple hydrolysis reaction.

This basic mechanism, as applied to reaction of *Z*-Gln-Gly and Gly-OMe, is shown in Scheme 2. According to this mechanism, *Z*-Gln-Gly combines with enzyme to form a Michaelis-complex from within which acylation of the sulfhydryl moiety of the active site Cys residue by the γ-amide functionality of the substrate occurs to form an acyl−enzyme intermediate. The acyl−enzyme then undergoes either hydrolysis to form *Z*-Glu-Gly or, if Gly-OMe is present, transamidation to form the isopeptide product *Z*-Glu-(GlyOMe)-Gly. Also shown in this mechanism is the binding of Gly-OMe to free enzyme to form a dead-end complex. Note that while this complex is not strictly required to explain these preliminary data, it is required to adequately model a complete data set (see below).

The steady-state rate equation that describes this mechanism is given in eq 1.

$$\frac{v_{ss}}{[E]} = \frac{k_c[S]}{K_m + [S]} = \frac{\left(\frac{k_s k_{deacyl}}{k_s + k_{deacyl}}\right)[S]}{K_s\left(1 + \frac{[N]}{K_n}\right)\left(\frac{k_{deacyl}}{k_s + k_{deacyl}}\right) + [S]} \quad (1)$$

where S is acyl-donor substrate *Z*-Gln-Gly, and N is nucleophile Gly-OMe. In addition,

$$k_{deacyl} = k'_w + k'_n \quad (2)$$

where

$$k'_w = \frac{k_w}{1 + \frac{[N]}{K_{na}}} \quad (3)$$

and

$$k'_n = \frac{k_{na}}{1 + \frac{K_{na}}{[N]}} \quad (4)$$

Since we observed that both k_c and K_m increase in the presence of Gly-OMe, we can conclude that k_s must be larger than both k'_w and k'_n (i.e., $k_s > k_{deacyl}$). This conclusion follows from simple inspection of eqs 1−4 which reveals that if k_s had been smaller than either of these constants, then neither k_c nor K_m would show a dependence on Gly-

OMe. This allows the simplification of eq 1 to

$$\frac{v_{ss}}{[E]} = \frac{k_{deacyl}[S]}{K_s\left(1 + \frac{[N]}{K_n}\right)\left(\frac{k_{deacyl}}{k_s}\right) + [S]} \quad (5)$$

or

$$\frac{v_{ss}}{[E]} = \frac{\frac{k_E}{1 + [N]/K_n}[S]\left(\frac{k_w}{1 + [N]/K_{na}} + \frac{k_{na}}{1 + K_{na}/[N]}\right)}{\frac{k_E}{1 + [N]/K_n}[S] + \frac{k_w}{1 + [N]/K_{na}} + \frac{k_{na}}{1 + K_{na}/[N]}} \quad (6)$$

where $k_E = k_s/K_s$. Equation 6 is a useful expression since while it is impossible from steady-state kinetic experiments to determine values for the individual mechanistic parameters k_s and K_s, it is possible to determine their mechanistically relevant ratio k_E.

To more thoroughly explore the applicability of this mechanism, we conducted an experiment in which we determined steady-state velocities for gpTGase-catalyzed reactions of a 2 × 2 matrix of six concentrations of *Z*-Gln-Gly (0.31 mM ≤ [*Z*-Gln-Gly] ≤ 10 mM) and seven concentrations of Gly-OMe (0 ≤ [Gly-OMe] ≤ 3 mM). The data from this study are plotted in Figure 1 in two ways: v_{ss}/[E] as a function of [*Z*-Gln-Gly] at constant concentrations of Gly-OMe (Figure 1A) and v_{ss}/[E] as a function [Gly-OMe] at constant concentrations of *Z*-Gln-Gly (Figure 1B).

Attempts at a global fit of the data to eq 6 did not converge until we made the assumption that over the range of Gly-OMe concentrations that we used, K_{na} > [Gly-OMe]. In this case, eq 6 now simplifies to

$$\frac{v_{ss}}{[E]} = \frac{\frac{k_E}{1 + [N]/K_n}[S]\left(k_w + \frac{k_{na}}{K_{na}}[N]\right)}{\frac{k_E}{1 + [N]/K_n}[S] + k_w + \frac{k_{na}}{K_{na}}[N]} \quad (7)$$

Best-fit values according to eq 7 are $k_E = 112\ M^{-1}\ s^{-1}$, $k_w = 0.16\ s^{-1}$, $k_{na}/K_{na} = 1800\ M^{-1}\ s^{-1}$, and $K_n = 7$ mM. These results are also summarized in Table 1 together with kinetic parameters for the other TGase reactions of this study.

Solvent Deuterium Isotope Effects for the gpTGase-Catalyzed Hydrolysis of Z-Gln-Gly. Table 2 summarizes the results of experiments in which we determined steady-state kinetic parameters for the gpTGase-catalyze hydrolysis of *Z*-Gln-Gly in H_2O and D_2O. In each solvent, two independent kinetic experiments were performed. The average values of the parameters and their associated error limits were used to calculate the following isotope effects as described in Table 2: $^D(k_c/K_m) = 0.45 \pm 0.03$ and $^Dk_c = 3.6 \pm 0.5$.

Reaction of N-Me-Casein with TGase. Using the GDH-coupled assay to monitor production of ammonia, we determined steady-state velocities at several concentrations of *N*-Me-casein. The data from four independent experiments are shown in Figure 2 and can be seen to adhere to a simple hyperbolic dependence of v_{ss}/[E] on [*N*-Me-casein]. Best-fit parameters according to the Michaelis−Menten equation are: $k_c = 0.14\ s^{-1}$, $K_m = 3.3\ \mu M$, and $k_c/K_m = 44\,000\ M^{-1}\ s^{-1}$.

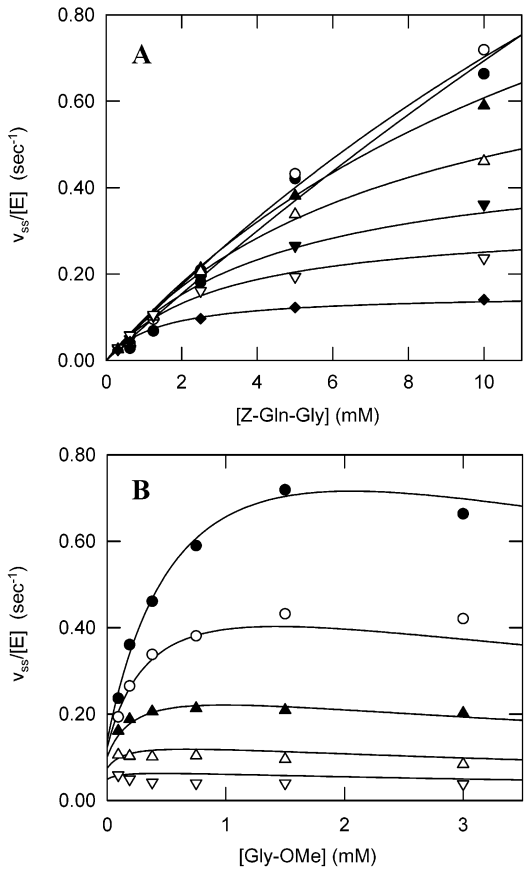

FIGURE 1: Steady-state kinetic experiment for the gpTGase-catalyzed transamidation of *Z*-Gln-Gly by Gly-OMe. (A) Dependence of v_{ss}/[E] on [*Z*-Gln-Gly] at seven fixed concentrations of Gly-OMe: 0 (◆), 0.094 (▽), 0.19 (▼), 0.38 (△), 0.75 (▲), 1.5 (○), and 3.0 (●) mM. (B) Dependence of v_{ss}/[E] on [Gly-OMe] at five fixed concentrations of *Z*-Gln-Gly: 0.63 (▽), 1.3 (△), 2.5 (▲), 5.0 (○), and 10 (●) mM. Steady-state velocities reflect rates of ammonia production determined in the GDH-coupled system described in the text. Each data point is the average of duplicate determinations. Lines through the data were drawn using the best-fit parameters of the global fit of the data to eq 7: $k_E = 112 \pm 6\ M^{-1}\ s^{-1}$, $k_w = 0.155 \pm 0.029\ s^{-1}$, $k_{na}/K_{na} = 1760 \pm 140\ M^{-1}\ s^{-1}$, and $K_n = 7.1 \pm 1.5$ mM. Reactions were conducted at 30 °C in a pH 7.4 buffer having the following composition: 50 mM HEPES, 500 mM NaCl, 10 mM $CaCl_2$, and 1 mM DTT. gpTGase concentration was 0.063 μM.

Figure 3 contains a progress curve for production of ammonia during reaction of 1 μM NMC (< $K_m = 3.3\ \mu M$) with 0.25 μM gpTGase. After the expected lag phase, the OD decreases exponentially with an observed pseudo-first-order rate constant of 0.133 min^{-1}. The total absorbance change at 340 nm is 0.0408 which corresponds to an ammonia production, or Gln consumption, of 6.6 μM ($\Delta\epsilon_{340} = -6200$). From triplicate determinations we calculate: $k_{obs} = 0.12 \pm 0.02\ min^{-1}$ and $\Delta[Gln] = 6.7 \pm 0.2\ \mu M$.

Cross-Linking Activity of gpTGase on Casein and N-Me-Casein. In Figure 4, time courses are shown for the gpTGase-catalyzed transpeptidation of casein and *N*-Me-casein. In these experiments, initial casein and *N*-Me-casein concentrations were approximately 50 μM. At the indicated times after addition of gpTGase, samples of the reaction mix were taken and analyzed electrophoretically.

TGase-Catalyzed Incorporation of Gly-OMe into N-Me-Casein. To study the transamidation of *N*-Me-casein by Gly-OMe, we used the GDH-coupled assay for ammonia

Table 1: Summary of Kinetic Constants for Reactions of Tissue Transglutaminase[a]

kinetic parameter	TGase reaction system			
	gpTGase *Z*-Gln-Gly Gly-OMe	gpTGase *N*-Me-casein Gly-OMe	gpTGase *N*-Me-casein DSC	hTGase *N*-Me-casein DSC
k_E (M^{-1} s^{-1})	110	97 000	64 000	26 000
k_u (s^{-1})[b]	0.16	0.16	0.14	0.13
k_u/k_E[c] (μM)	1400	1.6	2.3	5.1
K_n (μM)	7000	>1000	60	67
k_{na}/K_{na} (M^{-1} s^{-1})	1800	17 000	34 000	14 000
K_{na} (μM)	>3000	33	1.1	2.7
k_{na} (s^{-1})	>5	0.55	0.048	0.037

[a] All reactions conducted at 30 °C in a pH 7.4 buffer of 50 mM HEPES, 500 mM NaCl, 10 mM $CaCl_2$, and 1 mM DTT. [b] For reactions of *Z*-Gln-Gly, k_u corresponds to k_w of Scheme 2 and eqs 1−7. [c] This value is equivalent to K_m for substrate hydrolysis.

Table 2: Solvent Isotope Effects for GpTGase-Catalyze Hydrolysis of *Z*-Gln-Gly[a,b]

	k_c (s^{-1})	K_m (mM)	k_c/K_m (M^{-1} s^{-1})
H_2O	0.160	1.4	112
H_2O	0.168	1.6	100
D_2O	0.040	0.17	236
D_2O	0.052	0.22	240
^Dk	3.6 ± 0.5	7.7 ± 1.1	0.45 ± 0.03

[a] Kinetic parameters were determined from the fit to the Michaelis−Menten equation of the dependence of reaction velocity on substrate concentration at pH 7.4 and pD-equivalent (*34*) in a buffer of 50 mM HEPES, 500 mM NaCl, 10 mM $CaCl_2$, and 1 mM DTT at 30 °C. Enzyme concentration was 0.25 μM. [b] Two independent kinetic experiments were performed in H_2O and D_2O, respectively. Isotope effects, ^Dk, are the ratios of the means of parameters from the two kinetic experiments. Relative error was calculated using the expression: $[(\sigma_H)^2 + (\sigma_D)^2]^{1/2}$, where σ is the deviation from the mean; the absolute error reported in the table is the product of the mean and the relative error.

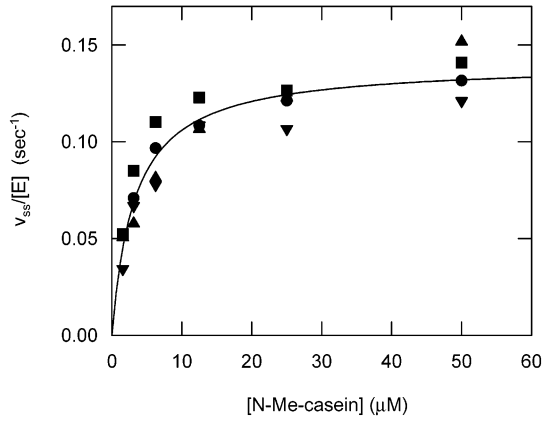

FIGURE 2: Steady-state kinetics of reaction of *N*-Me-casein with gpTGase. Steady-state velocities reflect rates of ammonia production determined in the GDH-coupled system described in the text. Data points represent four independent experiments. Best-fit parameters according to the Michaelis−Menten equation are $k_c = 0.140 \pm 0.004$ s^{-1}, and $K_m = 3.3 \pm 0.5$ μM. Reactions were conducted at 30 °C in a pH 7.4 buffer having the following composition: 50 mM HEPES, 500 mM NaCl, 10 mM $CaCl_2$, and 1 mM DTT. gpTGase concentration was 0.13 or 0.25 μM.

production to determine steady-state velocities as a function of Gly-OMe concentration at four fixed concentrations of *N*-Me-casein (5, 10, 20, and 40 μM). These data are shown in Figure 5 and were globally fit to eq 6 to provide the parameter estimates: $k_E = 97 \pm 8$ mM^{-1} s^{-1}, $k_w = 0.16 \pm 0.02$ s^{-1}, $k_{na} = 0.55 \pm 0.02$ s^{-1}; $K_{na} = 33 \pm 5$ μM, and $K_n > 1$ mM. Note that unlike the transamidation of *Z*-Gln-Gly, the data allowed us to estimate values of k_{na} and K_{na}.

TGase-Catalyzed Incorporation of Dansyl-Cadaverine into N-Me-Casein. To more conveniently study TGase-catalyzed

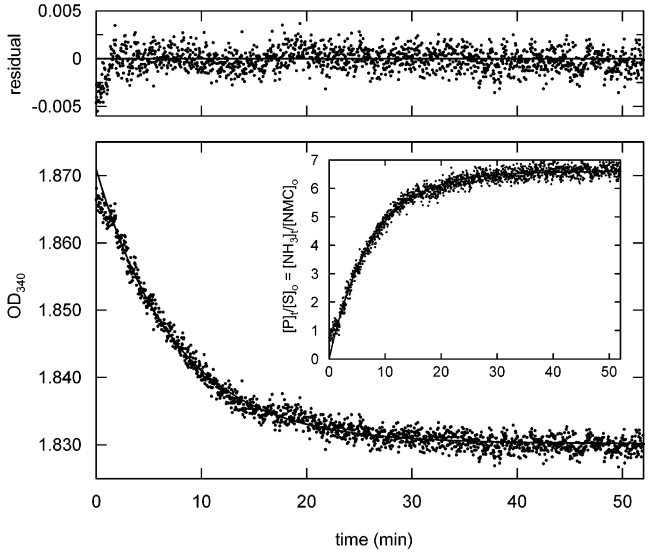

FIGURE 3: Progress curve for reaction of *N*-Me-casein with gpTGase. Using the GDH-coupled method for quantification of ammonia, the time course of reaction of 1 μM NMC with 0.25 μM gpTGase was followed. The data can be fit to the simple exponential decay: $OD_{340} = \Delta OD_{340}[\exp(-k_{obs}t)] + OD_{final}$. Best fit parameters are $k_{obs} = 0.133$ min^{-1}, $\Delta OD_{340} = 0.0408$, and $OD_{final} = 1.83$, and were used to draw the line through the data. The inset is the data expressed as the ratio of product concentration at time *t* to the initial substrate concentration. Reaction was conducted at 30 °C in a pH 7.4 buffer having the following composition: 50 mM HEPES, 500 mM NaCl, 10 mM $CaCl_2$, and 1 mM DTT.

transamidation of *N*-Me-casein by a low molecular weight nucleophile, we felt that we needed to develop an assay that gives rise to a signal that can be continuously monitored over time and is more sensitive than the GDH-coupled system. To this end, we took advantage of the increase in fluorescence intensity that is observed when dansyl-cadaverine is incorporated into protein substrates (*20*). Figure 6 shows progress curves collected on a fluorescence-plate reader for the TGase-catalyzed incorporation of DSC into *N*-Me-casein. From this data set, one can see that the maximum fluorescence intensity that is observed when all of the DSC has been incorporated into the protein is linearly dependent on DSC concentration with a slope of 133 ± 4 FI/μM DSC and a *y*-intercept of −7 ± 22 FI (see inset of Figure 6). Similar observations were made at several concentrations of *N*-Me-casein and allow us to calculate a proportionality factor of 137 ± 4 FI/μM DSC that can usedwhen converting steady-state velocities from units of FI/s to units of μM/s.

Another feature of these progress curves that validates the use of the observed fluorescence change as an accurate mea-

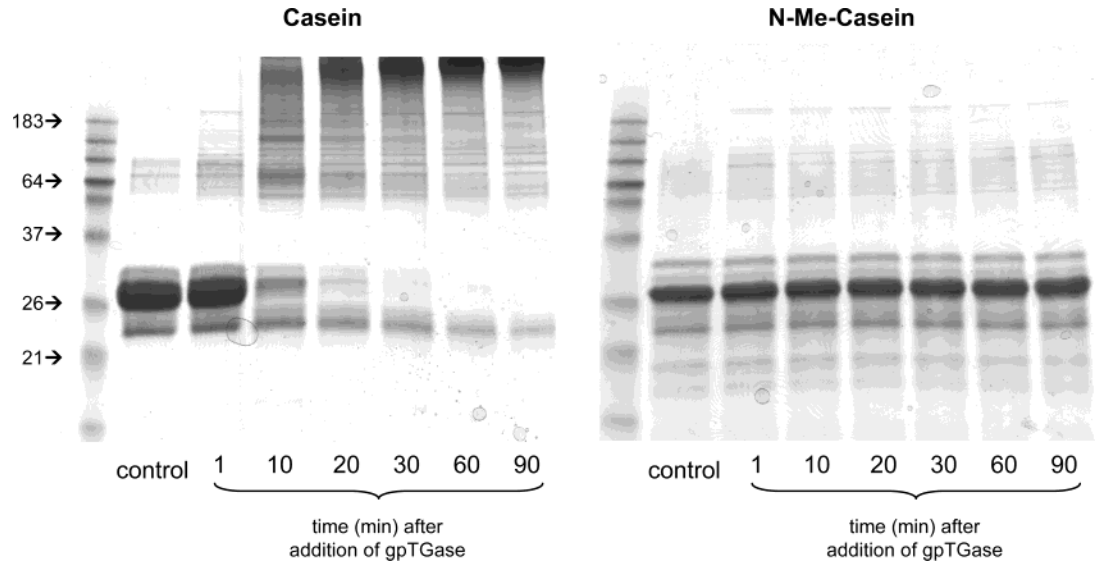

FIGURE 4: Time courses for the gpTGase-catalyzed transpeptidation of casein and *N*-Me-casein. Casein and *N*-Me-casein concentrations were approximately 50 μM. Control was substrate alone. At the indicated times, 100 μL aliquots were taken, boiled in SDS running buffer, and frozen at −20 °C until electrophoretic analysis. Reactions were conducted at 30 °C in a pH 7.4 buffer having the following composition: 50 mM HEPES, 500 mM NaCl, 10 mM $CaCl_2$, and 1 mM DTT. gpTGase concentration was 0.013 μM.

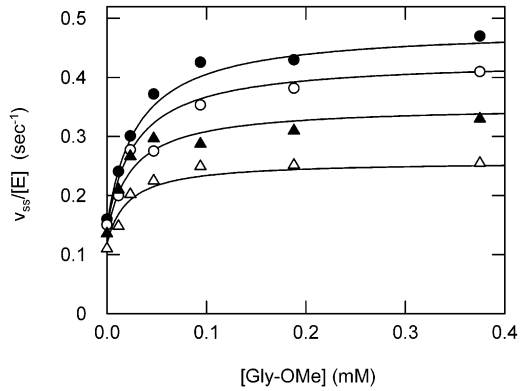

FIGURE 5: Steady-state kinetic experiment for the gpTGase-catalyzed transamidation of *N*-Me-casein by Gly-OMe. The plot shows the dependence of v_{ss}/[E] on [Gly-OMe] at four fixed concentrations of *N*-Me-casein: 5 (△), 10 (▲), 20 (○), and 40 (●) μM. Steady-state velocities reflect rates of ammonia production determined in the GDH-coupled system described in the text. Each data point is the average of duplicate determinations. Lines through the data were drawn using the best-fit parameters of the global fit of the data to eq 6: $k_E = 97 \pm 8$ mM^{-1} s^{-1}, $k_w = 0.16 \pm 0.02$ s^{-1}, $k_{na} = 0.55 \pm 0.02$ s^{-1}; $K_{na} = 33 \pm 5$ μM, and $K_n > 1$ mM. Reactions were conducted at 30 °C in a pH 7.4 buffer having the following composition: 50 mM HEPES, 500 mM NaCl, 10 mM $CaCl_2$, and 1 mM DTT. gpTGase concentration was 0.13 μM.

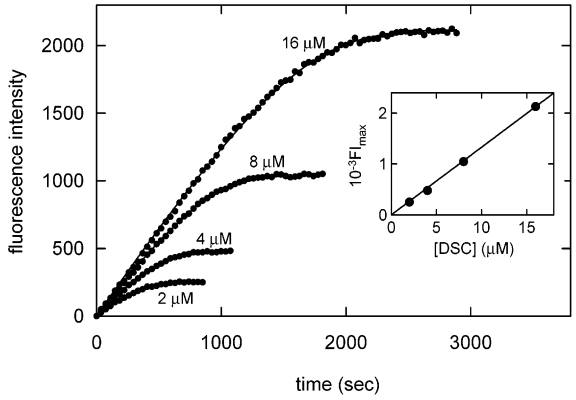

FIGURE 6: Progress curves for the TGase-catalyzed incorporation of dansyl-cadaverine into *N*-Me-casein. These reactions were conducted with [*N*-Me-casein] = 20 μM at the indicated DSC concentration and were monitored as the increase in fluorescence intensity FI at 500 nm ($\lambda_{ex} = 340$ nm). The data sets at each of the four DSC concentrations were fit to the integrated Michaelis−Menten equation to provide the following constants which were used to draw the lines through the data: 2 μM: $V_{max} = 1.78$ FI/s, $K_m = 297$ FI; 4 μM: $V_{max} = 1.49$ FI/s, $K_m = 236$ FI; 8 μM: $V_{max} = 1.46$ FI/s, $K_m = 245$ FI; and 16 μM: $V_{max} = 1.57$ FI/s, $K_m = 287$ FI. Reactions were conducted at 30 °C in a pH 7.4 buffer having the following composition: 50 mM HEPES, 500 mM NaCl, 10 mM $CaCl_2$, and 1 mM DTT. gpTGase concentration was 0.25 μM.

sure of transamidation by DSC is that they can be successfully fit to the integrated Michaelis−Menten equation. Values of V_{max} and K_m determined in this way are independent of the initial concentration of DSC (indicating an absence of product inhibition, enzyme inactivation, or other kinetic complexities) and provide the following parameter estimates averaged over the fitting results for the four curves: $V_{max} = 1.58 \pm 0.14$ FI/s and $K_m = 266 \pm 30$ FI. Using the conversion factor of 137 FI/μM and [E] = 0.25 μM, we can calculate $k_c = 0.046$ s^{-1} and $K_m = 1.9$ μM. These values agree with an analysis of the initial velocities of the data of Figure 6, where we find $k_c = 0.044$ s^{-1} and $K_m = 2.4$ μM, as well as with the more extensive steady-state analysis described below.

Kinetic Mechanism of the gpTGase-Catalyzed Transamidation of N-Me-Casein by Dansyl-Cadaverine. In these experiments, we determined steady-state velocities for gpTGase-catalyzed reactions of a 2 × 2 matrix at seven concentrations each of *N*-Me-casein (1.25 μM ≤ [NMC] ≤ 80 μM) and DSC (1.56 μM ≤ [DSC] ≤ 100 μM). Velocities at each of these substrate pairs were determined in duplicate or triplicate. Our method for analyzing these data is as follows.

At the each of the seven concentrations of *N*-Me-casein, we examined the dependence of v_{ss}/[E] on [DSC] and found that all seven of these dependencies exhibited substrate inhibition by DSC. These dependencies were individually fit to the general expression for substrate inhibition (*21*) of

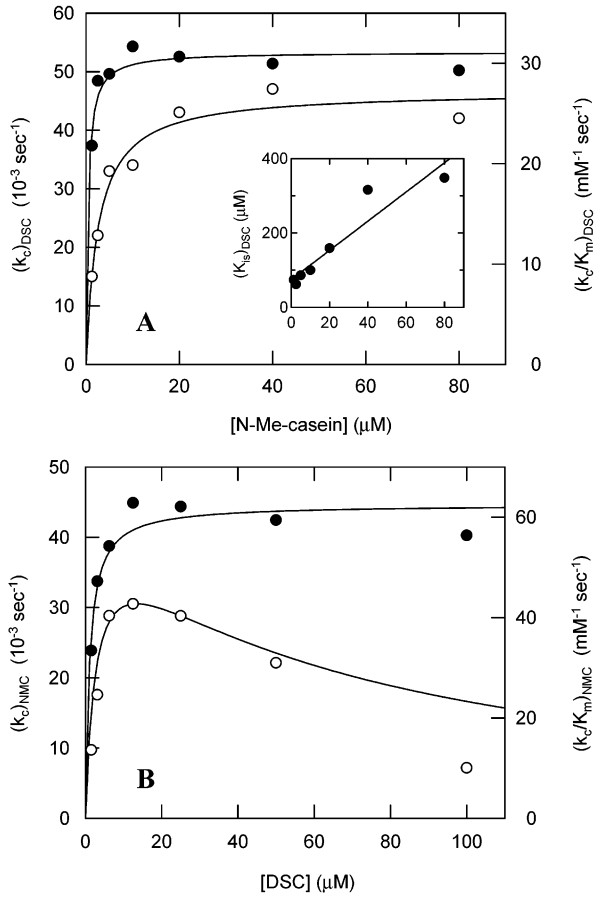

FIGURE 7: Analysis of steady-state rate data for the gpTGase-catalyzed transamidation of *N*-Me-casein by DSC. (A) [NMC]-dependent kinetic parameters. These parameters were determined from analysis of the dependence of v_{ss} on [DSC] at fixed concentrations of NMC. (B) [DSC]-dependent kinetic parameters. These parameters were determined from analysis of the dependence of v_{ss} on [NMC] at fixed concentrations of DSC. See text for details of analysis. In each panel, filled circles correspond to the *y*-axis on the left, while open circles correspond to the *y*-axis on the right. Reactions were conducted at 30 °C in a pH 7.4 buffer having the following composition: 50 mM HEPES, 500 mM NaCl, 10 mM $CaCl_2$, and 1 mM DTT. gpTGase concentration was 0.013 μM.

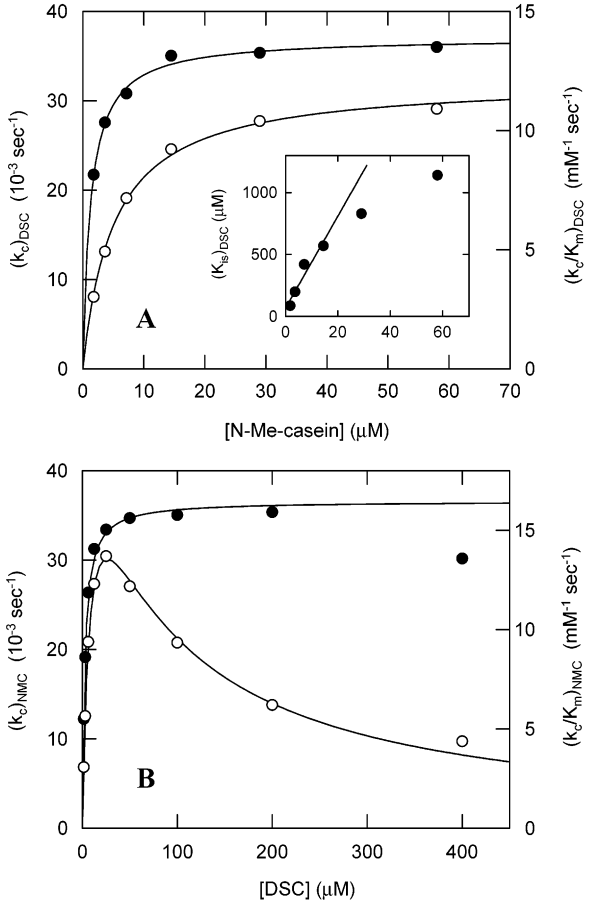

FIGURE 8: Analysis of steady-state rate data for the hTGase-catalyzed transamidation of *N*-Me-casein by DSC. (A) [NMC]-dependent kinetic parameters. These parameters were determined from analysis of the dependence of v_{ss} on [DSC] at fixed concentrations of NMC. (B) [DSC]-dependent kinetic parameters. These parameters were determined from analysis of the dependence of v_{ss} on [NMC] at fixed concentrations of DSC. See text for details of analysis. In each panel, filled circles correspond to the *y*-axis on the left, while open circles correspond to the *y*-axis on the right. Reactions were conducted at 30 °C in a pH 7.4 buffer having the following composition: 50 mM HEPES, 500 mM NaCl, 10 mM $CaCl_2$, and 1 mM DTT. hTGase concentration was 0.023 μM.

eq 8 to provide values of $(k_c)_{DSC}$, $(k_c/K_m)_{DSC}$, and $(K_{is})_{DSC}$

$$\frac{v_{ss}}{[E]} = \frac{\left\{\dfrac{(k_c)_{DSC}}{1 + [DSC]/(K_{is})_{DSC}}\right\}[DSC]}{\dfrac{(K_m)_{DSC}}{1 + [DSC]/(K_{is})_{DSC}} + [DSC]} \quad (8)$$

that were then plotted as a function of [*N*-Me-casein] as shown in Figure 7A. In contrast, at the each of the seven concentrations of DSC, we found that the dependencies of v_{ss}/[E] on [*N*-Me-casein] could be fit to the simple Michaelis−Menten equation to provide the values of $(k_c)_{NMC}$, and $(k_c/K_m)_{NMC}$ that are plotted in Figure 7B. As analyzed and discussed in detail below, these data are consistent with a transamidation mechanism that is similar to the mechanism of Scheme 2 for minimal substrates.

Kinetic Mechanism of the hTGase-Catalyzed Transamidation of N-Me-Casein by Dansyl-Cadaverine. In a series of experiments that were identical to those described for gpTGase, we determined steady-state kinetic parameters for the action of hTGase on *N*-Me-casein and DSC. The results of these experiments are shown in Figure 8 and can be interpreted in a mechanistic framework that is identical to the one developed for gpTGase (see below).

DISCUSSION

The principal goal of this study was to gain an understanding of the action of tissue transglutaminase on protein substrates, using casein and *N*,*N*-dimethylated casein as models. However, to build a conceptual framework for the interpretation of these studies, we felt it was essential to first investigate TGase-catalyzed reactions of the minimal substrate *Z*-Gln-Gly. The data we collected for reaction of TGase with both *Z*-Gln-Gly and *N*-Me-casein is consistent with the general established mechanism involving an acyl−enzyme intermediate that can decompose by pathways involving either reaction with water, to produce Glu-containing products, or a primary amine nucleophile, to produce an isopep-tide (*1*). Details of our mechanistic observations are discussed below.

Scheme 3: Minimal Mechanism for Cys/His Acyl-Transferases

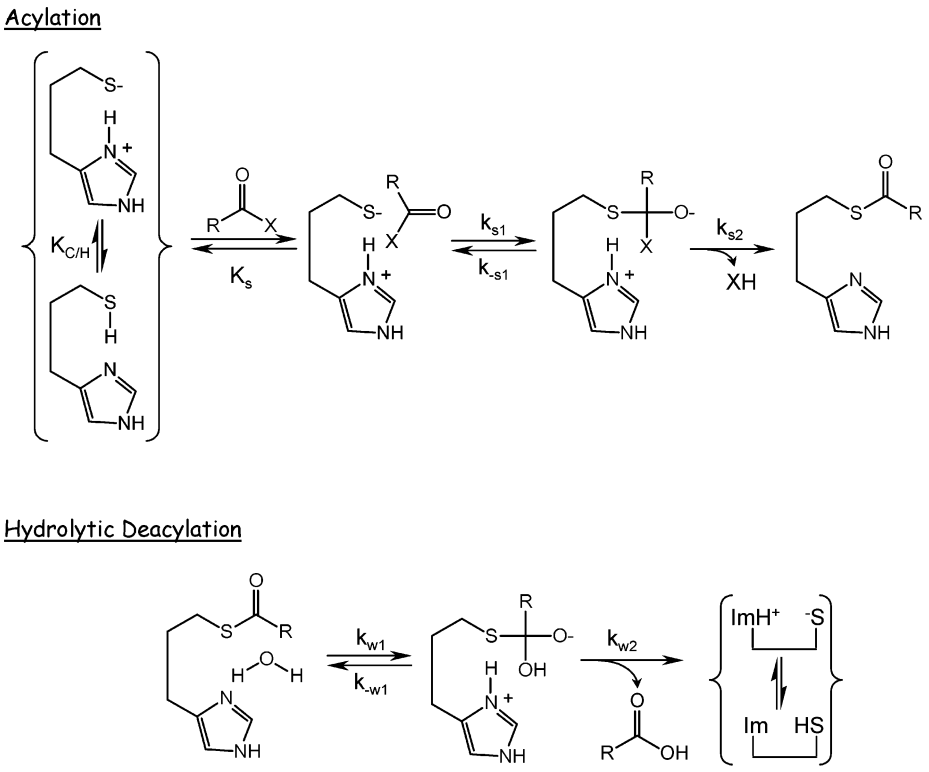

REACTIONS OF TISSUE TRANSGLUTAMINASE WITH THE MINIMAL SUBSTRATE Z-GLN-GLY.

In the absence of a suitable primary amine nucleophile, TGase catalyzes the simple hydrolysis of the minimal substrate *Z*-Gln-Gly to produce *Z*-Glu-Gly and ammonia. When nucleophiles, such as Gly-OMe, are added to reaction solutions of TGase and *Z*-Gln-Gly, the acyl−enzyme intermediate undergoes aminolysis, giving rise to the isopeptide product *Z*-Glu(γ-GlyOMe)-Gly. Two interesting features emerge from our kinetic analyses of these reactions: (i) Acylation of the active site thiol by the primary amide of *Z*-Gln-Gly is more rapid than deacylation of the resultant thioester acylenzyme (i.e., $k_s > k_w$, see Scheme 2). While this is contrary to chemical expectations, it is well supported by the TGase literature and has precedent in studies of serine proteases, aryl acylamidase, and γ-glutamyl transpeptidase (*22*−*26*). (ii) TGase is able to bind nucleophile in a manner that is not catalytically productive as suggested by the observations of substrate inhibition that is seen not only during reaction of *Z*-Gln-Gly with Gly-OMe (Figure 1) but also during reaction of *N*-Me-casein with dansyl-cadaverine catalyzed by both the guinea pig and human enzymes (Figures 5 and 6, respectively).

To explore the hydrolytic reaction in more detail, we determined solvent deuterium isotope effects (see Table 2) and found the following: $^{D}(k_c/K_m) = 0.45 \pm 0.03$ and $^{D}k_c = 3.6 \pm 0.5$.[2] These isotope effects are reminiscent of the solvent isotope effects that are observed for reactions of papain and other hydrolases and acyl-transferase that are mechanistically related to TGase in that they all possess active site Cys/His diads (*27*−*33*). In all of these cases, $^{D}(k_c/K_m)$ values range from inverse effects around 0.4 to slightly normal effects of 1.1, while $^{D}k_c$ values are usually large and normal and range from 1.5 to 3.5.

We will first consider the solvent isotope effect of 0.45 on k_c/K_m for the hydrolysis of *Z*-Gln-Gly by gpTGase. In the upper half of Scheme 3 is the minimal mechanism for the manifold of reaction steps governed by k_c/K_m for TGase and other Cys/His acyl-transferase. According to this mechanism for acylation, the active site Cys/His diad exists as tautomers, SH/Im and S^-/ImH^+, whose equilibrium is governed by $K_{C/H}$ (= [SH/Im]/[S^-/ImH^+]). Note that the Michaelis-complex, S^-/ImH^+:R−C(O)X, can form by either of two routes: (i) direct binding of substrate to S^-/ImH^+, or (ii) binding of substrate to SH/Im followed by rapid proton transfer to form S^-/ImH^+:R−C(O)X which then collapses to the acyl−enzyme with release of leaving group XH. Formation of the tetrahedral intermediate is thought to occur by nucleophilic attack by the thiolate anion on the carbonyl carbon of the substrate with no catalytic assistance by general acids or bases. In the final step of the acylation manifold, the tetrahedral intermediate collapses to form the acyl−enzyme with expulsion of leaving group XH. For amine leaving groups, this step is thought to be subject to general acid catalysis by the imidazolium cation of the active site His.

The rate expression for k_c/K_m according to this mechanism is given in eq 9.

$$k_c/K_m = \frac{\left(\frac{k_{s1}k_{s2}}{k_{-s1} + k_{s2}}\right)}{K_s(1 + K_{C/H})} \qquad (9)$$

[2] In a study of gpTGase-catalyzed hydrolysis of *Z*-Glu(γ-*p*-nitrophenyl ester)-Gly, solvent isotope effects were reported to be $^{D}(k_c/K_m) = 4.2$ and $^{D}k_c = 1.0$ (*35*). It is unclear why these values are so different from those reported here or how to interpret them within the mechanistic framework that has emerged from the study of thiohydrolase catalysis and solvent isotope effects (see below).

Scheme 4: Origins of Solvent Deuterium Isotope Effects

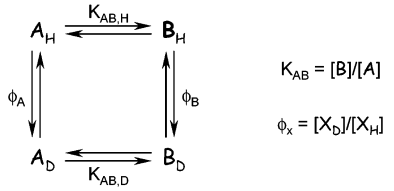

In the derivation of this equation, we assumed that substrate can only bind to the reactive form of the enzyme, S^-/ImH^+. An equivalent expression can, of course, be written for the situation where substrate binds to SH/Im. The isotope effect on k_c/K_m is a complex function of the isotope effects on the individual equilibrium and rate constants: ${}^DK_{C/H}$, ${}^DK_s$, ${}^Dk_{s1}$, ${}^Dk_{-s1}$, and ${}^Dk_{s2}$. One way to proceed here is to first consider the likely magnitudes of each of these individual isotope effects.

First, consider the general case of Scheme 4 in which A and B are in equilibrium and, further, both A and B have one exchangeable hydrogen. The solvent deuterium isotope effect on K_{AB} is expressed in eq 10 as the ratio of hydrogen fractionation factors (*34*) for

$$ {}^DK_{AB} = \frac{K_{AB,H}}{K_{AB,D}} = \frac{\phi_A}{\phi_B} \tag{10}$$

the two species that are in equilibrium. If A and B have several exchangeable hydrogenic sites, eq 10 becomes:

$$ {}^DK_{AB} = \frac{\prod_i \phi_{A,i}}{\prod_j \phi_{B,j}} \tag{11}$$

where *i* and *j* are the number exchangeable hydrogenic sites on A and B, respectively.

Likewise, solvent deuterium isotope effects on rate constants can be expressed as

$$ {}^Dk = \frac{\prod_i \phi_{r,i}}{\prod_j \phi_{\neq,j}} \tag{12}$$

where $\phi_{r,i}$ and $\phi_{\neq,j}$ are fractionation factors for the exchangeable hydrogens in the reactant and transition state, respectively, of the reaction under consideration.

Cys/His acyl-transferases are generally thought to possess only two exchangeable hydrogenic sites with nonunity fractionation factors: the thiol moiety of the active site Cys residue and the protonic bridge that forms between reacting moieties of enzyme and substrate in transition states of general acid/base-catalyze reaction steps (*34*). The fractionation factor for the thiol hydrogen is 0.4, while values for the protonic bridges formed during protolyic catalysis can range from 0.6 to 0.2, with a typical average value of about 0.3 (*34*). Given this, we can assign the following rough estimates to the solvent isotope effects for the five discrete reactions steps of Scheme 3:

$$ {}^DK_{C/H} = \phi_{S^-/ImH^+}/\phi_{SH/Im} = 1/0.4 = 2.5 \tag{13}$$

$$ {}^DK_s = \phi_{S^-/ImH^+}/\phi_{E:acylX} = 1 \tag{14}$$

$$ {}^Dk_{s1} = \phi_{E:acylX}/\phi_{\neq,s1} = 1 \tag{15}$$

$$ {}^Dk_{-s1} = \phi_{TI}/\phi_{\neq,-s1} = 1 \tag{16}$$

$$ {}^Dk_{s2} = \phi_{TI}/\phi_{\neq,s2} = 1/0.3 = 3.3 \tag{17}$$

With these estimates of isotope effects on individual reactions, it is possible to calculate estimates of the overall isotope effect on k_c/K_m for the four limiting cases of eq 9. These are summarized in Table 3.

From this analysis, it is clear that that our observed isotope effect on k_c/K_m of 0.45 results from a situation similar to limiting case IV of Table 3. Thus, for the gpTGase-catalyzed hydrolysis of *Z*-Gln-Gly, we propose that the Cys/His diad exists predominantly as the neutral SH/Im species and that acylation is rate-limited by attack of the thiolate on the carbonyl carbon of the γ-amide moiety of *Z*-Gln-Gly.

We can perform a similar analysis of the solvent isotope effect on k_c. First recall that for the gpTGase-catalyzed hydrolysis of *Z*-Gln-Gly, $k_s > k_w$ (see Scheme 2) and, thus, $k_c = k_w$ (see eq 1, [N] = 0). Like acylation, hydrolysis of the acyl−enzyme proceeds through a tetrahedral intermediate (see Scheme 3). k_w has the following form:

$$ k_w = \frac{k_{w1}k_{w2}}{k_{-w1} + k_{w2}} \tag{18}$$

Estimates of the solvent isotope effects for the three individual steps is done as above. While estimates of ${}^Dk_{w1}$and ${}^Dk_{-w1}$ are straightforward as outlined in eqs 19 and 20 since

$$ {}^Dk_{w1} = \phi_{acyl}/\phi_{\neq,w1} = 1/0.3 = 3.3 \tag{19}$$

$$ {}^Dk_{-w1} = \phi_{TI}/\phi_{\neq,w1} = 1/0.3 = 3.3 \tag{20}$$

the transition states for these two steps must involve general catalysis, the estimate of ${}^Dk_{w2}$ is not as clear. We see then, that in this case it is difficult to predict whether decomposition of the tetrahedral intermediate to products will involve general acid assisted departure of thiolate by the imidazolium cation or if thiolate will depart unassisted. Given this, $\phi_{\neq,w2}$ might vary from 0.3 to 1 and our estimates of ${}^Dk_{w2}$ vary as

$$ {}^Dk_{w2} = \phi_{TI}/\phi_{\neq,w2} = 1/1 - 1/0.3 = 1 - 3 \tag{21}$$

Our observation of an isotope effect on k_c of 3.6, therefore, does not allow us to decided which step is rate-limiting. All we can say at present is that in the transition state for k_w a proton bridge has been established with a fractionation factor of about 0.28.

KINETIC ANALYSIS OF REACTIONS OF TISSUE TRANSGLUTAMINASE WITH N-ME-CASEIN.

In this section, we will provide an analysis of the steady-state kinetic experiments that were conducted with TGase and the protein substrate *N*-Me-casein. Before this analysis, two general comments should be made. First, despite the potential for unmanageable kinetic complexity in this system, it should be noted that the kinetics of reaction of TGase with

Table 3: Estimates of Solvent Isotope Effects on k_c/K_m for Cys/His Acyl-Transferases According to the General Mechanism of Scheme 6

limiting case	$^{D}(k_c/K_m)$	estimate
case I: $K_{C/H} \ll 1$; $k_{-s1} \gg k_{s2}$	$\dfrac{\left(\dfrac{^{D}k_{s1}}{^{D}k_{-s1}}\right)^{D} k_{s2}}{^{D}K_s}$	3.3
case II: $K_{C/H} \ll 1$; $k_{-s1} \ll k_{s2}$	$\dfrac{^{D}k_{s1}}{^{D}K_s}$	1.0
case III: $K_{C/H} \gg 1$; $k_{-s1} \gg k_{s2}$	$\dfrac{\left(\dfrac{^{D}k_{s1}}{^{D}k_{-s1}}\right)^{D} k_{s2}}{^{D}K_s\,^{D}K_{C/H}}$	1.3
case IV: $K_{C/H} \gg 1$; $k_{-s1} \ll k_{s2}$	$\dfrac{^{D}k_{s1}}{^{D}K_s\,^{D}K_{C/H}}$	0.4

N-Me-casein are, in fact, tractable. The fact that this reaction can be subjected to standard steady-state kinetic analysis allows it to become the basis of an assay to discover inhibitors of TGase and motivates us to proceed with studies of the action of TGase on tau, huntingtin, and other aggregating proteins of neurodegenerative diseases. Second, gpTGase and hTGase follow identical kinetic mechanisms with nearly identical kinetic parameters for the mechanistic rate constants (see Table 1). Given the 80% overall homology between the two enzymes (*35*) and the identity of the region flanking the active site Cys (*36*), this may not be entirely surprising. A practical consequence of this kinetic identity is that it justifies the use of commercially available gpTGase in drug discovery programs involving either mechanism-based inhibitor design or screening.

Enzymatic Reaction of Protein Substrates − General Considerations. Clearly, enzymatic reactions of protein substrates will reflect processes that are different from those of enzymatic reaction of simple peptide substrates. Interpretation of the former will always need to be informed by a variety of mechanistic factors; some general and some specific to the enzyme. In the present case, we need to consider three factors: (i) initial velocity kinetics of nonprocessive enzymatic reaction of polymeric substrates, (ii) extent of Lys-derivitization in substrate *N*-Me-casein, and (iii) modes of deacylation of TGase acyl-enzymes. For the latter two factors, we will be specifically concerned with the action of TGase in the absence of exogenous nucleophile (see Figures 2 and 3).

(i) Several classes of enzyme catalyze nonprocessive chemical modification at multiple sites on a polymeric substrate. For protein substrates, these enzymes include proteases, kinases, phosphatases, and, of course, transglutaminases. For reaction of these enzymes with their protein substrates, the kinetic situation is usually more complex than for reaction with peptidic substrates containing only a single functionality that the enzyme recognizes. Apparent steady-state kinetic parameters that are measured for turnover of protein substrates will be complex functions of the microscopic kinetic parameters for reaction of the enzyme with each of the individual functionalities. For example, consider the general mechanism of Scheme 5 where

Scheme 5: Minimal Mechanism for Nonprocessive Reaction of an Enzyme with a Polyfunctional Substrate

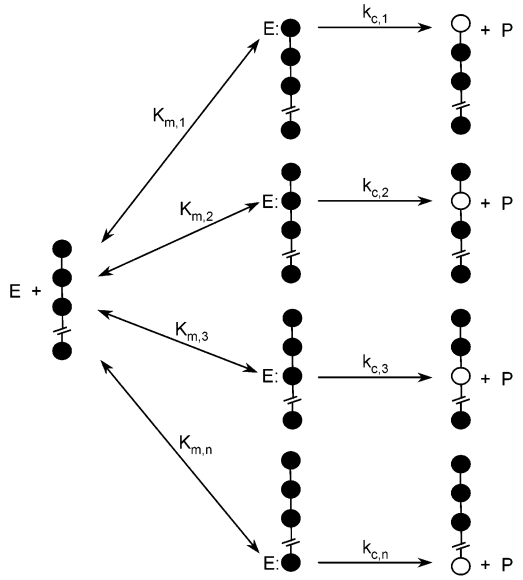

enzyme is seen to bind substrate in *n* different ways to produce *n* catalytically competent Michaelis complexes which all turnover to produce their unique product as well as a product P that all pathways have in common.[3] Initial velocities for production of common product P show a simple hyperbolic dependence on substrate concentration:

$$\frac{d[P]}{dt} = \frac{k_c[E]_o[S]_o}{K_m + [S]_o} \tag{22}$$

where

$$K_m = \left(\sum_{i=1}^{n} \frac{1}{K_{m,i}}\right)^{-1} \tag{23}$$

$$k_c = \sum_{i=1}^{n} k_{c,i} \frac{K_m}{K_{m,i}} \tag{24}$$

and

$$\frac{k_c}{K_m} = \sum_{i=1}^{n} \left(\frac{k_c}{K_m}\right)_i \tag{25}$$

Thus, for an enzymatic reaction that follows the mechanism of Scheme 5, simple Michaelis−Menten kinetics will be observed. K_m will be the reciprocal of the sum of reciprocals over all individual values of $K_{m,i}$ and predominantly reflect dissociation of the Michaelis-complex of greatest stability. k_c will the sum over all individual $k_{c,i}$, where each is multiplied by a factor $K_m/K_{m,i}$ that gives weight to turnover of the Michaelis-complex of greatest stability.

[3] Note that the mechanism of Scheme 5, and eqs 22−25, hold only for initial velocities where production of P reflects turnover of substrate and not turnover of the *n* products, which themselves can, of course, serve as substrates. The kinetic scheme for complete turnover of all reactive functionalities of a polymeric substrate is more complex. If the various rate constants differ appreciably among themselves, one can anticipate multiphasic progress curves for production of P. This is discussed below.

Finally, for this mechanism, the observed value of k_c/K_m is the simple summation over all values of $(k_c/K_m)_i$.

We see then that the values of k_c and K_m that we determined for reaction of gpTGase with *N*-Me-casein (Figure 2) may reflect contributions from multiple parallel pathways. However, despite this kinetic complexity, we will usually be able to interpret results of our kinetic experiments as if TGase combines with *N*-Me-casein to form a single Michael-complex. Implicit in these interpretations is the understanding that multiple Michaelis-complexes likely form.

(ii) While the preceding is general and holds for all nonprocessive enzymatic reactions of polymeric substrates, one of two factors that apply specifically to reactions of TGase is the extent to which the Lys residues *N*-Me-casein have been derivatized. The *N*-Me-casein that we used in these studies is a commercial product in which purified, bovine casein[4] had been subjected to reductive methylation to dimethylate Lys residues. Amino acid analysis demonstrated that of the 14 Lys residues in native casein, only 3−5 were modified (data not shown). The kinetic consequence of this modification is shown in Figure 4 which contains time courses for the gpTGase-catalyzed transpeptidation of casein and *N*-Me-casein.

Figure 4 clearly demonstrates that in the presence of gpTGase, casein is shifted to successively higher molecular weight species, indicating that casein undergoes gpTGase-catalyzed intermolecular transpeptidation. In contrast, *N*-Me-casein undergoes no shift in molecular weight. Together with the data of Figure 2, which indicate that the action of gpTGase liberates ammonia from *N*-Me-casein, these data suggest that reactions of gpTGase with *N*-Me-casein are limited to Gln hydrolysis and/or intramolecular transpeptidation. Thus, despite the fact that *N*-Me-casein contains 9−11 unmethylated Lys residues, it must be the case that those residues that are methylated are those that in native casein react in intermolecular transpeptidation reactions. The increased reactivity of this population of Lys residues in native casein toward both reductive methylation and TGase-catalyzed transpeptidation is presumably due to either their greater solvent exposure or to an enhanced inherent chemical reactivity or both.

(iii) The other TGase-specific feature we will discuss here is modes of deacylation. The ideas to be discussed are illustrated in Scheme 6 where a general mechanism is provided for the reaction of TGase with a protein substrate. In this scheme, E is TGase, S is protein substrate, E−acyl is the acyl−enzyme formed from reaction of the active site Cys with one of the protein's Gln residues, S−S is the isopeptide product formed from intermolecular reaction of E−acyl with a Lys residue on a second molecule of substrate, and S′ is the sum of hydrolysis and intramolecular isopeptide products

Scheme 6: Mechanistic Proposal for Reaction of *N*-Me-Casein with TGase

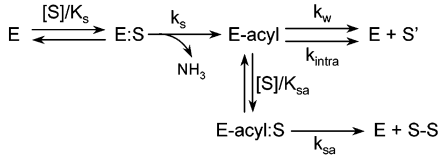

that form from unimolecular deacylation of E−acyl. For this mechanism,

$$\frac{v_{ss}}{[E]} = \frac{\left(\frac{k_s k_{deacyl}}{k_s + k_{deacyl}}\right)[S]}{K_s\left(\frac{k_{deacyl}}{k_s + k_{deacyl}}\right) + [S]} \quad (26)$$

where

$$k_{deacyl} = \frac{k_{sa}}{1 + K_{sa}/[S]} + \frac{k_w}{1 + [S]/K_{sa}} + \frac{k_{intra}}{1 + [S]/K_{sa}} \quad (27)$$

Now, as we have seen (Figure 4), *N*-Me-casein does not undergo gpTGase-catalyzed intermolecular transpeptidation. This indicates that either k_{sa} is very small or that K_{sa} is very large, or both. Since it is also the case that unmodified casein *does* undergo intermolecular transpeptidation, it is reasonable to assume that *N*-Me-casein can bind to E−acyl with an affinity similar to that of casein; that is, K_{sa} for casein and *N*-Me-casein are similar in magnitude. Thus, we can conclude that *N*-Me-casein does not undergo intermolecular transpeptidation due to a small value of k_{sa}. k_{sa} for *N*-Me-casein is small presumably due to the methylation of the 3−5 reactive and/or accessible Lys residues. A low value of k_{sa} allows eq 27 (and thus eq 26) to be simplified to the following:

$$k_{deacyl} = \frac{k_w}{1 + [S]/K_{sa}} + \frac{k_{intra}}{1 + [S]/K_{sa}} \quad (28)$$

Further simplification of eq 28 can be made based on the observation in Figure 2 that substrate inhibition was not observed. This suggests that K_{sa} is much larger than 50 μM and therefore $[S]/K_{sa} \ll 1$. Equation 26 now becomes:

$$\frac{v_{ss}}{[E]} = \frac{\left(\frac{k_s k_u}{k_s + k_u}\right)[S]}{K_s\left(\frac{k_u}{k_s + k_u}\right) + [S]} \quad (29)$$

where k_u is the sum of the two unimolecular modes of deacylation:

$$k_u = k_w + k_{intra} \quad (30)$$

Finally, if like *Z*-Gln-Gly, acylation is rapid relative to deacylation for reaction of *N*-Me-casein with gpTGase (and this gains experimental support below), eq 29 can be further simplified to

[4] This casein (Sigma, C-5890) is a mixture of α_{s1} (45%), α_{s2} (12%), β (33%), and κ (10%) caseins. While it is almost axiomatic in enzymology that one should only conduct detailed kinetic and mechanistic studies with well-defined, pure substrates, this axiom does not hold for nonprocessive enzymes acting on protein substrates in which the enzyme-reactive functionalities of the substrate are (i) distributed randomly along the primary sequence of the protein and (ii) embedded in local environments of varying primary sequence. In the context of the mechanism of Scheme 5, this means that it is irrelevant if all *n* is contained within a single species (for example, if we were using only β-casein) or if *n* is distributed among several species, as it is here.

$$\frac{v_{ss}}{[E]} = \frac{k_u[S]}{K_s\left(\frac{k_u}{k_s}\right) + [S]} \quad (31)$$

We see then that for reaction of *N*-Me-casein with gpTGase, the k_c value of 0.14 s^{-1} reflects deacylation of E−acyl by the two parallel routes of hydrolysis and intramolecular transpeptidation. The K_m value of 3 μM is not a simple dissociation constant reflecting the stability of the Michaelis-complex E:S, but rather contains a kinetic term, k_u/k_s, that reflects partitioning of the acyl−enzyme and thus the stability of E−acyl.

TGase-Catalyzed Transamidation of N-Me-Casein by Dansyl-Cadaverine. Examination of Figure 7A,B suggests the mechanism of Scheme 7 where S′ and S−N correspond to *N*-Me-casein-derived products originating from either unimolecular decomposition of the E−acyl enzyme via k_u or from reaction with dansyl-cadaverine via k_{na}. The rate equation that describes the mechanism of Scheme 7 is given in eq 32.

$$\frac{v_{ss}}{[E]} = \frac{k'_E[S]\left(\frac{k_{na}[N]}{K_{na} + [N]}\right)}{k'_E[S] + k_u' + \frac{k_{na}[N]}{K_{na} + [N]}} \quad (32)$$

where

$$k'_E = \frac{k_E}{1 + [N]/K_n} \quad (33)$$

and

$$k'_u = \frac{k_u}{1 + [N]/K_{na}} \quad (34)$$

Equation 32 can be rearranged in two ways to analyze the two plots of Figure 7. When substrate *N*-Me-casein is varied at constant concentrations of nucleophile DSC, the [DSC]-dependent parameters of Figure 7B are generated and eq 35 is used for analysis.

$$\frac{v_{ss}}{[E]} = \frac{\left(\frac{k_{na}[N]}{K_{na} + [N]}\right)[S]}{K_s(1 + [N]/K_n)\left(\frac{k_n[N]}{K_{na} + [N]} + \frac{k_u}{1 + [N]/K_{na}}\right) + [S]} \quad (35)$$

In this expression, we see that the dependence of $(k_c)_{NMC}$ on [DSC] is governed by

$$(k_c)_{NMC} = \frac{k_{na}[N]}{K_{na} + [N]} \quad (36)$$

while the dependence of $(k_c/K_m)_{NMC}$ on [DSC]can be shown to be governed by

Scheme 7: Mechanistic Proposal for Reaction of TGase-Catalyzed Transamidation of *N*-Me-Casein by Dansyl-Cadaverine

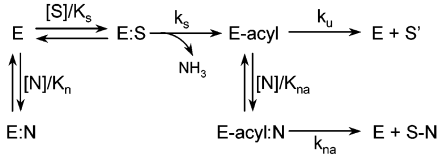

$$(k_c/K_m)_{NMC} = \frac{k_E}{\left(1 + \frac{[N]}{K_n}\right)\left(1 + \frac{k_u}{k_{na}}\frac{K_{na}}{[N]}\right)} \quad (37)$$

When the dependence of $(k_c)_{NMC}$ on [DSC] of Figure 7B is analyzed according to eq 36, the following best fit parameters are obtained: $k_{na} = 0.0448 \pm 0.0016$ s^{-1}, $K_{na} = 1.1 \pm 0.2$ μM, and $k_{na}/K_{na} = 40.8 \pm 1.2$ mM^{-1} s^{-1}. Likewise, when the dependence of $(k_c/K_m)_{NMC}$ on [DSC] of Figure 7B is analyzed according to eq 37 with $(k_{na}/K_{na})^{-1}$ constrained to 40.8 mM^{-1} s^{-1}, we find: $k_E = 64 \pm 12$ mM^{-1} s^{-1}, $K_n = 61 \pm 12$ μM, and $k_u = 0.136 \pm 0.024$ s^{-1}.

When nucleophile DSC is varied at constant concentrations of substrate *N*-Me-casein, the [NMC]-dependent parameters of Figure 7A are generated. To analyze these data, eq 32 is rearranged to produce eq 38.

$$\frac{v_{ss}}{[E]} = \frac{\left\{\frac{\frac{k_{na}}{1 + K_{m,n}/[S]}}{1 + \frac{[N]}{K_n(1 + [S]/K_{m,n})}}\right\}[N]}{K_{na}\left\{\frac{1 + \frac{K_{m,u}}{[S]}(1 + [N]/K_n)}{1 + \frac{K_{m,n}}{[S]}(1 + [N]/K_n)}\right\} + [N]} \quad (38)$$

where

$$K_{m,n} = \frac{k_{na}}{k_E} \quad (39)$$

and

$$K_{m,u} = \frac{k_u}{k_E} \quad (40)$$

Eq 38 predicts that at increasingly larger concentrations of N, reaction velocities will be driven to zero by the a [S]-dependent inhibition term that is equal to

$$(K_{is})_{DSC} = K_n\left(1 + \frac{[S]}{K_{m,n}}\right) \quad (41)$$

Eq 38 predicts a linear dependence of $(K_{is})_{DSC}$ on [NMC], and this is what is observed in the inset of Figure 7A. The slope of the line through the data is K_n and equals 74 ± 22 μM, while the intercept is $K_n/K_{m,n}$ and equals 3.9 ± 0.1.

The $(k_c)_{DSC}$-term of eq 38 is also [S]-dependent and is expressed in eq 42:

$$(k_c)_{DSC} = \frac{k_{na}}{1 + K_{m,n}/[S]} \quad (42)$$

Fitting the data of Figure 7A to eq 42 provides the following: $k_{na} = 0.0532 \pm 0.016\ s^{-1}$ and $K_{m,n} = 0.42 \pm 0.11\ \mu M$.

As concentrations of N approach zero, eq 38 reduces to

$$\left(\frac{k_c}{K_m}\right)_{DSC} = \frac{k_{na}/K_{na}}{1 + K_{m,w}/[S]} \quad (43)$$

which expresses the [S]-dependence of $(k_c/K_m)_{DSC}$. The best fit parameters of the data of Figure 7A are $k_{na}/K_{na} = 27.2 \pm 1.2\ mM^{-1}\ s^{-1}$ and $K_{m,w} = 2.6 \pm 0.5\ \mu M$.

Kinetic analysis of the data for reaction of the human enzyme (Figure 8) proceeds identically to the above. The rate constants from this analysis are summarized in Table 1.

MECHANISTIC FEATURES OF REACTIONS OF TISSUE TRANSGLUTAMINASE WITH N-ME-CASEIN.

Examination of Table 1 brings to light three kinetic situations that deserve mechanistic interpretation: (i) k_E ($= k_s/K_s$) is 200−1000 times larger for acylation of TGase by *N*-Me-casein than for acylation by *Z*-Gln-Gly, (ii) k_u values are identical and equal 0.15 s^{-1} for all four reactions, and (iii) k_{na}/K_{na} is sensitive to both the structure of the substrate-derived portion of the acyl−enzyme as well as to the amine nucleophile.

Kinetics of Acylation of TGase by Minimal and Protein Substrates. As we just saw in the discussion surrounding Scheme 5 and eqs 22−25, the kinetics of action of TGase on NMC can be anticipated to be more complex than the enzyme's action on *Z*-Gln-Gly. At the very least, there is the purely statistical issue of how to deal with the fact that any kinetic parameter measured for reaction of NMC will necessarily reflect reaction with some portion of the protein's Gln residues. We must therefore first address this statistical problem before we can consider the issue of the enzyme's selectivity toward its substrates.

Our progress curve analysis (Figure 3) allows us to calculate the number of Gln residues that can react with gpTGase and indicates that about seven of NMC's 14 Gln residues (*37*) are catalytic competent for acyl-transfer to gpTGase. In the context of the mechanism of Scheme 5, this means that $n = 7$. It is unclear why only seven of the total 14 Gln residues are reactive toward gpTGase. The lack of reactivity of the remaining Gln residues is likely related to the structural features (I°, II°, or III°) of their local protein environment.

Now, these progress curves were determined under the condition [NMC] < K_m, which, for simple systems, allows simplification of rate laws such that progress curves are pseudo-first-order in substrate concentration with observed rate constant equal to $(k_c/K_m)[E]$. Interestingly, the progress curves determined here for acylation of gpTGase by NMC can be described by a simple first-order rate-law (see Figure 3) with $k_{obs} = 0.12\ min^{-1}$. Such simplicity was unanticipated, given the complex kinetic mechanism that must certainly obtain for enzymatic turnover of the seven Gln residues.

Simulations of a more tractable system, with $n = 3$, demonstrate that an exponential dependence of [P] on time

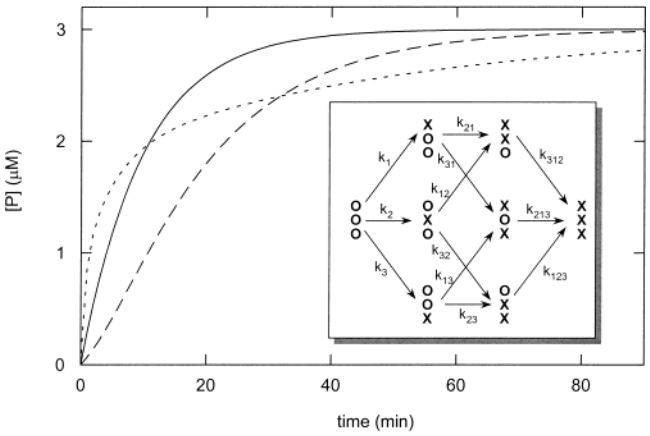

FIGURE 9: Simulated progress curves for nonprocessive enzymatic turnover of a polymeric substrate with three reactive functionalities. In the model for the simulations (see inset): (1) each arrow represents enzymatic turnover of one functionality (○) to product (**X**) under pseudo-first-order conditions (i.e., [S] < K_m), with release of one equivalent of product P per turnover (for clarity, P is not explicitly shown in the model), and (2) each rate constant k_x reflects the corresponding product $(k_c/K_m)_x[E]_{total}$. In the model the solid line $k_x = k_{xx} = k_{xxx} = 0.1$; dashed line: $k_x = 0.02$, $k_{xx} = 0.1$, $k_{xxx} = 0.5$; and, dotted line: $k_x = 0.5$, $k_{xx} = 0.1$, $k_{xxx} = 0.02$.

will only be observed if all rate constants of the system are of similar magnitude; differences greater than a factor of 2 or 3 among rate constants result in progress curves with multiple kinetic phases. Examples of such simulations are shown in Figure 9 where three limiting cases are considered. Such simulations also demonstrate that when all the rate constants of the system are the same (i.e., when all rate constants equal $(k_c/K_m)_x[E]_{total}$), the observed rate constant will be equal to this value. For example, the solid line of Figure 9 is the simulated progress curve for enzymatic turnover of a polymeric substrate with three reactive functionalities for which all rate constants of the system have a value of 0.1. This curve is perfectly fit by a simple first-order rate law with rate constant equal to 0.1.

When applied to the present case, this means that the k_{obs} value of 0.12 min^{-1} for reaction of gpTGase with NMC reflects a complex mechanism in which reaction of each of the seven Gln residues is governed by a $(k_c/K_m)_x$ value is approximately equal to $(0.12\ min^{-1})/[E]_{total;}$ or 8000 $M^{-1}\ s^{-1}$.

Significantly, $(k_c/K_m)_x$ is identical to $(k_c/K_m)_i$ derived from our initial velocity analysis. Recall from eq 25 that k_c/K_m is a composite value equal to the simple summation over all values of $(k_c/K_m)_i$. In the present case, k_c/K_m has been determined in three independent initial velocity experiments: 44 $mM^{-1}\ s^{-1}$ (see Results section *Reaction of NMC with TGase*), 97 $mM^{-1}\ s^{-1}$ (k_E in Table 1 for transamidation of NMC by Gly-OMe), and 64 $mM^{-1}\ s^{-1}$ (k_E in Table 1 for transamidation of NMC by DSC). The average value is 68 ± 27 $mM^{-1}\ s^{-1}$. If we now assume that $(k_c/K_m)_i$ values for all seven Gln residues are approximately the same, than $(k_c/K_m)_i = k_c/K_m/n = (68\ mM^{-1}\ s^{-1})/7 = 9.7 \pm 3.9\ mM^{-1}\ s^{-1}$, which and is identical, within error, to the $(k_c/K_m)_x$ of 8 $mM^{-1}\ s^{-1}$.

$(k_c/K_m)_x$ can be compared with values of k_c/K_m for reaction TGase with simple peptides. From our studies, we see an 80-fold increase in catalytic efficiency for reaction of gpTGase with *Z*-Gln-Gly ($k_c/K_m = 100\ M^{-1}\ s^{-1}$) relative to reaction with NMC ($(k_c/K_m)_x = 8000\ M^{-1}\ s^{-1}$). Significantly, this is essentially identical to the 100-fold increase observed

Scheme 8: Aminolysis of Acyl-Enzymes Derived from Transglutaminase

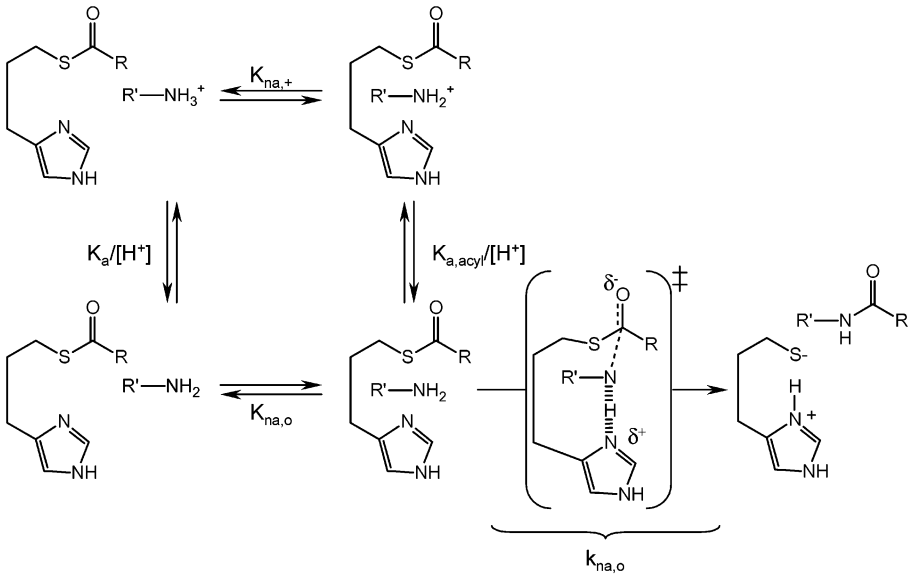

by Piper et al. (*17*) for reaction of hTGase with *Z*-Gln-Gly (42 M^{-1} s^{-1}) relative to reaction with the specific wheat gliadin peptide Pro-Gln-Pro-Gln-Leu-Pro-Tyr-Pro-Gln-Pro-Gln-Leu-Pro-Tyr (4800 M^{-1} s^{-1}; underlined Gln residue is primary site of reaction). This suggests that the catalytically important interactions between TGase and NMC are probably restricted to the active site region and argues against the presence of an exo-site region on the enzyme surface that might have been involved in interactions with remote regions of the protein substrate. Thus, it appears that a Gln residue in the context of a protein has no greater reactivity toward TGase than does a Gln residue in a peptide of appropriate sequence. However, we cannot rule out the possibility that certain, highly specific protein substrates may, in fact, interact with TGase in binding modes that are not available to NMC and thereby manifest greater reactivity.

Hydrolysis of Acyl−Enzymes Derived from Reaction of Gln-Donors with TGase. The identity of k_u values for the four hydrolytic deacylation reactions reported in this study (see Table 1) is reminiscent of the situation that is observed for serine hydrolases (*38* and references therein) where, depending on the protease, identical or nearly identical rate constants are obtained for hydrolyses of acyl−enzymes derived from substrates of varying peptide length. Like the situation here, this indicates that TGase's selectivity toward it substrates is not manifested in hydrolytic deacylation, but rather in acylation. Why this should be so, and why this should be so for acyl-transferases as structurally unrelated as serine hydrolases and TGases, is not entirely clear at this time. But we can offer the following speculation, based in part on our recent study of α-chymotrypsin catalysis (*38*).

We propose that these enzymes all operate by a mechanism that, during the reaction of hydrolytic deacylation, is characterized by compensation between the enthalpy and entropy of activation. One can imagine that as substrates are elaborated into structures that are recognized as specific substrates by the enzyme (for example, in proceeding from *Z*-Gln-Gly to protein substates for TGase and from Suc-Phe-pNA to Suc-Ala-Ala-Pro-Phe-pNA for α-chymotrypsin), that these changes might allow additional enthalpically favorable interactions to be established. If these interactions are manifested to a disproportionately greater degree in the acyl−enzyme than the transition state for deacylation, we would actually observe a decrease in rate as the substrates become more specific. However, in such a mechanism, we can also reasonably expect that values of $-T\Delta S^{\ddagger}$ would decrease as specificity requirements are fulfilled since reaching the transition state from the acyl−enzyme for the more specific will require less organization. We see then that according to this mechanism, acyl−enzymes of specific substrates are simultaneously enthalpically stabilized and preorganized for deacylation. The compensatory nature of these two effects results in deacylation rates that can be relatively insensitive to structure of the acyl−enzyme (*38*).

Aminolysis of Acyl-Enzymes of TGase. Another finding of this study that deserves analysis is the observation that k_{na}/K_{na} is sensitive to both the structure of the substrate-derived portion of the acyl−enzyme as well as to the amine nucleophile. The principle observation we will explore here is for gpTGase where we have a more complete data set and is that k_{na}/K_{na} for reaction of DSC with the acyl−enzyme derived from NMC is 17 times larger than k_{na}/K_{na} for reaction of Gly-OMe with the acyl−enzyme derived from *Z*-Gln-Gly (Table 1). As detailed below, this rate constant disparity arises from a combination of two factors: (i) the difference in nucleophilic reactivity between Gly-OMe and DSC, and (ii) the difference in structure of acyl−enzyme undergoing aminolysis.

The starting point for analysis is Scheme 8 which depicts the likely mechanism of aminolysis of acyl−enzymes derived from TGase. This mechanistic proposal is based on nonenzymatic aminolysis of thioesters (*39*−*42*), and the results of this and other studies on TGase (*1*, *43*). A critical mechanistic feature that is depicted in this scheme is that aminolysis must proceed from within a Michaelis-complex in which both the amine and imidazole moiety of the active site His are in their basic forms. The former is required for nucleophilic reaction with the thioester acyl−enzyme and the latter for general-base catalysis of this nucleophilic attack.

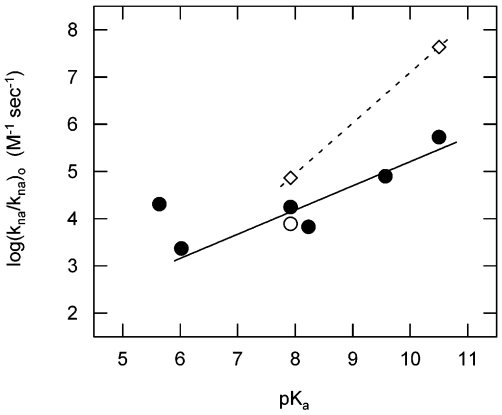

FIGURE 10: Dependence of log(k_{na}/K_{na})$_o$ on amine pK_a for aminolysis of acyl−enzymes derived from gpTGase. Filled symbols correspond to data from Leblanc et al. (*43*) (nucleophile, pK_a: aminoacetonitrile, 5.6; trifluorethylamine, 6.0; Gly-OMe, 7.9; Gly-NH_2, 8.2; 2-(ethylthio)ethylamine, 9.6; Ac-Lys-OMe, 10.5. pH 7.0 buffer: 100 mM MOPS and 50 mM $CaCl_2$, 25 °C) while open symbols are from this study (pH 7.4 buffer: 50 mM HEPES, 500 mM NaCl, 10 mM $CaCl_2$, and 1 mM DTT, 30 °C). In both cases, circles correspond to reaction of nucleophile with acyl-enzyme derived from *Z*-Gln-Gly. Diamonds to reaction of Gly-OMe (pK_a = 7.9) or dansyl-cadaverine (pK_a = 10.5) with *N*-Me-casein. (k_{na}/K_{na})$_o$ calculated from k_{na}/K_{na} using eq 45.

Equation 44 describes a form of the rate law for this mechanism in which only the basic form of

$$\frac{v_{ss}}{[E]} = \frac{k_{na,o}[R'NH_2]}{K_{na,o} + [R'NH_2]} = \frac{k_{na,o}[R'NH_2]_{total}}{K_{na,o}\left(1 + \frac{[H^+]}{K_a}\right) + [R'NH_2]_{total}} \quad (44)$$

the amine can bind to the acyl−enzyme. A kinetically equivalent version can of course be written in which $R'NH_3^+$ binds and subsequently loses a proton before nucleophilic attack.

Equation 45 is a rearranged form of eq 44 that allows us to convert observed values of k_{na}/K_{na}

$$\left(\frac{k_{na}}{K_{na}}\right)_o = \left(\frac{k_{na}}{K_{na}}\right)\{1 + 10^{pK_a - pH}\} \quad (45)$$

into values of (k_{na}/K_{na})$_o$, the second-order rate constant for reaction of acyl−enzyme with the basic form of the amine, $R'NH_2$. Expressing these rate constants as (k_{na}/K_{na})$_o$ values allows us to analyze the influence of nucleophile basicity on acyl−enzyme reactivity toward nucleophiles and gain some understanding of the transition state for this process.

Now, one way to analyze the sensitivity of a nucleophilic addition reaction to nucleophilic reactivity is examine the dependence of log(k_o) on pK_a of the conjugate acid of the nucleophile, where k_o is the second-order rate constant for attack of the basic form of the nucleophile. A graphical representation of this dependence constitutes a Brønsted plot and, in the absence of complicating factors, should be linear with slope, designated β_{nuc}, that reflects the development of positive charge on the nucleophile in the transition state (*40*, *41*).

Figure 10 is a Brønsted plot for aminolysis of acyl−enzymes derived from reaction of gpTGase and was constructed using data from this study and a study by Keillor and co-workers (*43*). In this plot, three outliers are apparent: the data point for aminolysis by aminoacetonitrile (pK_a = 5.6) and the data points for aminolysis by Gly-OMe (pK_a = 7.9) and DSC (pK_a = 10.5) of the acyl−enzyme derived from *N*-Me-casein.

Other than these three reactions, which we consider below, the aminolysis reactions under consideration are well described by a Brønsted relationship with a β_{nuc} value of 0.51 ± 0.07. A β_{nuc} value of this magnitude suggests a modest degree of positive charge build-up on the attacking nitrogen and is consistent with the transition state structure shown in Scheme 8 in which this charge would be delocalized to the imidazole moiety as well as to the attacking amine. It is significant that these nucleophiles, which differ substantially in their structures, fall on the same correlation line suggesting that reactivity toward acyl−enzyme is largely controlled by nucleophilic strength and not structural determinants. Given this, it is some of some interest to discuss the outliers in the plot.

The positive departure of aminoacetonitrile from the linear correlation suggests that reaction of acyl−enzyme with aminoacetonitrile is proceeding by an alternate, faster pathway. Several possibilities exist for this pathway, including general-base catalysis by aminoacetonitrile of water attack on the acyl−enzyme. Since this would produce *Z*-Glu-Gly instead of the anticipated *Z*-Glu(γ-aminoacetonitrile)-Gly, an analysis of products would be diagnostic here.

The other two outliers corresponds to reaction of Gly-OMe and dansyl-cadaverine with the acyl−enzyme derived from *N*-Me-casein and define a line with slope β_{nuc} of 1. A β_{nuc} of unity indicates a transition state for aminolysis in which covalent bond formation between the nitrogen of the attacking amine and the carbonyl carbon of the thioester acyl−enzyme is well advanced of proton transfer to the imidazole moiety of the active site His residue (or some other base). It is unclear how aminolysis mechanism can be so dramatically sensitive to acyl−enzyme structure. Clearly, additional data will have to be collected if we want to make the case for a mechanism in which nucleophilic reactivity, as reflected in β_{nuc}, is sensitive and dependent on the structure of the acyl−enzyme.[5]

SUMMARY

In this paper, we have presented results of kinetic studies of the action of tissue transglutaminase on the protein substrate *N*-Me-casein. The kinetics of this reaction are amenable to study by the standard analytic apparatus of enzyme kinetics and have allowed a number of mechanistic conclusions to be drawn: (i) catalytically important interactions between TGase and NMC are restricted to the active site and do not involve interactions at remote sites on the enzyme surface, (ii) hydrolysis of acyl−enzymes, derived from both peptide and protein substrates, proceeds with identical rate constants and supports a mechanism involving compensation between the enthalpy and entropy of activation (*38*), and (iii) the transition state for aminolysis of acyl−

[5] These experiments are underway and support a β_{nuc} value that is, in fact, sensitive to acyl-enzyme structure. Preliminary, unpublished results for TGase-catalyzed aminolysis of NMC by N- and C-blocked analogues of Lys (pK_a = 10.5) indicate values of k_{na}/K_{na} that are nearly identical to those for reaction with DSC (pK_a = 10.5; k_{na}/K_{na} = 30 400 M^{-1} s^{-1}).

enzymes of TGase involves protolytic catalysis and the degree of proton transfer in the transition state is sensitive not only nucleophile basicity but also to structural features of the Gln-donor substrate.

In the future, we will see if these conclusions extend to the action of TGase on tau, huntingtin, α-synuclein, and other causative proteins of neurodegenerative disorders and go on to use this knowledge to discover drugs for the treatment of these diseases (*44*).

REFERENCES

1. Folk, J. E. (1983) *Adv. Enzymol. Relat. Areas Mol. Biol. 44*, 1−56.
2. Folk, J. E., and Chung, S. (1985) *Methods Enzymol. 113*, 358−375.
3. Copper, A. J. L., Jeitner, T. M., and Blass, J. P. (2002) *Neurochem. Int. 40*, 1−5.
4. Kim, S. Y., Jeitner, T. M., and Steinert, P. M. (2002) *Neurochem. Int. 40*, 85−103.
5. Lesort, M., Tucholski, J., Miller, M. L., and Johnson, G. V. W. (2000) *Prog. Neurobiol. 61*, 439−463.
6. Sarvari, M., Fesus, L., and Nemes, Z. (2002) *Drug Dev. Res. 56*, 458−472.
7. Singer, S. M., Zainelli, B. M., Norlund, M. A., Lee, J. M., and Muma, N. A. (2002) *Neurochem. Int. 40*, 17−30.
8. Miller, M. L., and Johnson, G. V. W. (1995) *J. Neurochem. 65*, 1760−1770.
9. Johnson, G. V. W., Cox, T. M., Lockhart, J. P., Zinnerman, M. D., Miller, M. L., and Powers, R. E. (1997) *Brain Res. 751*, 323−329.
10. Junn, E., Ronchetti, R. D., Quezado, M. M., Kim, S. Y., and Mouradian, M. M. (2003) *Proc. Natl. Acad. Sci. U.S.A. 100*, 2047−2052.
11. Mastroberardino, P. G., Iannicola, C., Nardacci, R., Bernassola, F., DeLaurenzi, V., Melino, G., Mereno, S., Pavone, F., Oliverio, S., Fesus, L., and Piacentini, M. (2002) *Cell Death Differ. 9*.
12. Karpuj, M. V., Becher, M. W., Springer, J. E., Chabas, D., Youssef, S., Pedott, R., Mitchell, D., and Steinman, L. (2002) *Nat. Med. 8*, 143−149.
13. Cooper, A. J. L., Jeitner, T. M., Gentile, V., and Blass, J. P. (2002) *Neurochem. Int. 40*, 53−67.
14. Jeitner, T. M., Bogdanov, M. B., Matson, W. R., Daikhin, Y., Yudkoff, M., Folk, J. E., Steinman, L., Browne, S. E., Beal, M. F., Blass, J. P., and Cooper, A. J. L. (2001) *J. Neurochem. 79*, 1109−1112.
15. de Cristofaro, T., Affaitati, A., Cariello, L., Avvedimento, E. V., and Varrone, S. (1999) *Biochem. Biophys. Res. Commun. 260*, 150−158.
16. Gentile, V., Sepe, C., Calvani, M., Melone, A. B. M., Cotrufo, R., Cooper, A. J. L., Blass, J. P., and Peluso, G. (1998) *Arch. Biochem. Biophys. 352*, 314−321.
17. Piper, J. L., Gray, G. M., and Khosla, C. (2002) *Biochemistry 41*, 396−393.
18. Day, N., and Keillor, J. W. (1999) *Anal. Biochem. 274*, 141−144.
19. Cleland, W. W. (1979) *Anal. Biochem. 99*, 142−145.
20. Lorand, L., Siefring, G. E., Tong, Y. S., Bruner-Lorand, J., and Gray, A. J. (1979) *Anal. Biochem. 93*, 453−458.
21. Copeland, R. A. (2000) in *Enzymes − A Practical Introduction to Structure, Mechanism, and Data Analysis*, pp 137−138, Wiley-VCH, New York, NY.
22. Stein, R. L. (2002) *Biochemistry 41*, 991−1000.
23. Stein, R. L. (2001) *Biochemistry 40*, 5804−5811.
24. Rahfeld, J., Schutkowski, M., Faust, J., Neubert, K., Barth, A., and Heins, J. (1991) *Biol. Chem. Hoppe-Seyler 372*, 313−318.
25. Stein, R. L., Viscarello, B. R., and Wildonger, R. A. (1984) *J. Am. Chem. Soc. 106*, 796−798.
26. Hedstrom, L., Lin, T. Y., and Fast, W. (1996) *Biochemistry 35*, 4515−4523.
27. Whitaker, J. R., and Bender, M. L. (1965) *J. Am. Chem. Soc. 87*, 2728−2737.
28. Frankfater, A., and Kuppy, T. (1981) *Biochemistry 20*, 5517−5524.
29. Weiss, P. M., Cook, P. F., Hermes, J. D., and Cleland, W. W. (1987) *Biochemistry 26*, 7378−7384.
30. Brocklehurst, K., Kowlessur, D., Patel, G., Templeton, W., Quigley, K., Thomas, E. W., Wharton, C. W., Willenbrock, F., and Szawelski, R. J. (1988) *Biochem. J. 250*, 761−762.
31. Hanzlik, R. P., Zygmunt, J., and Moon, J. B. (1990) *Biochim. Biophys. Acta 1035*, 62−70.
32. Born, T. L., and Blanchard, J. S. (1999) *Biochemistry 38*, 14416−14423.
33. Rudolph, J. (2002) *Biochemistry 41*, 14613−14623.
34. Quinn, D. M., and Sutton, L. D. (1991) in *Enzyme Mechanism from Isotope Effects* (Cook, P. F., Ed.) pp 73−126, CRC Press, Boston, MA.
35. Gentile, V., Saydak, M., Chiocca, A. E., Akande, O., Birckichler, P. J., Lee, K. N., Stein, J. P., and Davies, P. J. A. (1992) *J. Biol. Chem. 266*, 478−483.
36. Chen, J. S. K., and Mehta, K. (1999) *Int. J. Biochem. Cell Biol. 31*, 817−836.
37. Goda, S. K., Sharman, A. F., Yates, M., Mann, N., Carr, N., Minton, N. P., and Brehm, J. K. (2000) *Appl. Microbiol. Biotechnol. 54*, 671−676.
38. Case, A., and Stein, R. L. (2003) *Biochemistry 42*, 3335−3348.
39. Bruice, T. C., and Benkovic, S. (1966) in *Bioorganic Mechanisms*, pp 259−297, W. A. Benjamin, Inc., New York.
40. Jencks, W. P. (1969) in *Catalysis in Chemistry and Enzymology*. pp 72; 537−542, McGraw-Hill Book Co., New York.
41. Castro, E. A. (1999) *Chem. Rev. 99*, 3505−3524.
42. Yang, W. (2000) *Org. Lett. 2*, 4133−4136.
43. Leblanc, A., Gravel, C., Labelle, J., and Keillor, J. W. (2001) *Biochemistry 40*, 8335−8342.
44. Stein, R. L. (2003) *Drug Discovery Today 8*, 245−248.

BI030084Z